ELSEVIER

Journal of Structural Geology 29 (2007) 1811–1830

JOURNAL OF STRUCTURAL GEOLOGY

www.elsevier.com/locate/jsg

# Kinematic and geometric analysis of fault-related folds in a rift setting: The Dannemarie basin, Upper Rhine Graben, France

M. Ford [a,*], C. Le Carlier de Veslud [a], O. Bourgeois [b]

[a] *Centre de Recherche Petrographiques et Geochimiques (CRPG, UPR2300 CNRS), ENSG-INPL, 15 rue ND des Pauvres, BP 20, 54501 Vandoeuvre-lès-Nancy, France*

[b] *Université de Nantes, Laboratoire de Planétologie et Géodynamique, 2 rue de la Houssinière, B.P. 92208, 44322 Nantes, France*

Received 12 December 2006; received in revised form 1 August 2007; accepted 5 August 2007
Available online 14 August 2007

**Abstract**

The Upper Rhine Graben (URG) developed in the Alpine foreland from mid-Eocene to Pliocene as part of the West European rift system. The Dannemarie basin occupies the SW termination of the URG and is bordered by the Vosges fault zone (west) and the Illfurth fault zone (east). We constructed a 3D model of faults and principal pre- and syn-rift stratigraphic surfaces, using all available subsurface and surface geological and geophysical data. The model shows: (1) syn-rift strata thinning across kilometre-scale, fault-parallel, monoclinal flexures associated with basin margin faults; and (2) major basin-margin faults terminating laterally into major flexures. Sequential cross-section restorations show that these flexures accommodated deposition of over 1300 m of syn-rift strata (Salt Series which is 42–63% of the basin fill). These folds are interpreted as syn-rift fault-propagation folds that developed above normal faults. Their geometry is replicated in a trishear numerical model using reasonable parameter values. Fold development was controlled principally by: (1) reactivation of favourably oriented basement faults; (2) the presence of a thick viscous layer (principally Triassic evaporites) allowing decoupling between crystalline basement and competent Jurassic cover; and (3) a relatively slow deformation rate.


*Keywords:* Upper Rhine Graben; Dannemarie Basin; Rift; Extensional fault-propagation folds; Trishear; Basement-cover decoupling

## 1. Introduction

Several studies have recognised the role of extension-related folds in accommodating subsidence during rifting by using seismic data in the Norwegian and North Seas (Withjack et al., 1990; Young et al., 2001), offshore Nova Scotia, Canada (Keller and Lynch, 1999) and the Gamtoos Basin of South Africa (Paton and Underhill, 2004), and field studies of young rifts such as the Gulf of Suez (Sharp et al., 2000; Gawthorpe et al., 2003), and the Upper Rhine Graben (Laubscher, 1982; Larroque and Ansart, 1985; Maurin, 1995; Maurin and Nivière, 2000). Analogue and numerical modelling can reproduce extension-related folds, described either as fault-propagation folds or forced folds (Withjack et al., 1990; Vendeville et al., 1995; Hardy and McClay, 1999; Withjack and Callaway, 2000; Finch et al., 2004; Hardy and Finch, 2006). Models show folds forming as upward widening zones of distributed deformation above discrete faults at depth. With increasing displacement, the fault cuts through the fold as it propagates upward, leaving a footwall anticline and a hanging-wall syncline. Numerical kinematic models, in particular trishear, can replicate such fold development in extension (e.g. Allmendinger, 1998; Hardy and McClay, 1999; Zehnder and Allmendinger, 2000; Khalil and McClay, 2002; Jin and Groshong, 2006). These folds typically (but not exclusively) develop in the presence of a distinct competence contrast between strong basement and sedimentary cover or when a significant viscous layer is present between rigid basement and overlying cover. Both analogue experiments (Vendeville

* Corresponding author.
*E-mail address:* mford@crpg.cnrs-nancy.fr (M. Ford).

0191-8141/$ - see front matter © 2007 Elsevier Ltd. All rights reserved.
doi:10.1016/j.jsg.2007.08.001

et al., 1995; Withjack and Callaway, 2000) and recent discrete-element-method mechanical models (Hardy and Finch, 2006) incorporating strong competence contrasts indicate that, in some cases, cover deformation is not localized above the active fault but is distributed across a much wider area.

Numerous authors have described folds along the faulted margins of the Tertiary Upper Rhine Graben (URG), (Laubscher, 1982; Maurin, 1995; Maurin and Nivière, 2000; Giamboni et al., 2004; Le Carlier de Veslud et al., 2005; Rotstein et al., 2005a,b; Ustaszewski et al., 2005). Some authors propose that such folds record a late Alpine transpressional event (Nivière and Winter, 2000; Rotstein et al., 2005a). Based on the geometric relationship between syn-rift stratigraphy and the folds, other authors (Maurin and Nivière, 2000; Ustaszewski et al., 2005; Le Carlier de Veslud et al., 2005) recognise them as syn-rift forced folds that developed above basement-cutting normal faults. In this paper, we present a multidisciplinary study of folds associated with basin bounding faults in the Guebwiller area of the Vosges fault zone and on both sides of the Dannemarie basin, the southernmost depocentre of the URG (Figs. 1 and 2). We show that these folds developed principally during early rifting. They may however have accommodated some minor late reactivation. Our aims are to clarify and, where possible, quantify: (1) their 2D and 3D geometry, timing and distribution using, in particular, the relationship between syn-rift stratigraphy and folding; (2) the parameters that controlled fold development; and (3) the interplay between folding and faulting.

All available geophysical and geological data were complied within the 3D geo-modeller gOcad (Mallet, 2002), including some 50 seismic reflection lines. These data were used to construct a 3D geometrical model of major fault surfaces and stratigraphic horizons and isopach maps of synrift strata. Syn-rift growth strata were then used to sequentially restore key cross-sections. These restorations in turn constrained trishear models using the FaultFold software (Allmendinger, 1998; Zehnder and Allmendinger, 2000). Comparison of results with published analogue and numerical experiments provides insight into the processes and parameters that controlled folding in this setting.

## 2. The Dannemarie basin

### 2.1. Tectonic setting

The URG forms part of the West-European Tertiary rift system (Sittler, 1969, 1983; Illies, 1975; Ziegler, 1992; Merle and Michon, 2001). Initiation of the NNE-SSW oriented Rhine Graben (Fig. 1) is not well constrained with estimates of latest Priabonian (36 Ma; Sissingh, 1998,2003) or Lutetian (42.5 Ma; Berger, 2005a,b) being proposed. The graben developed principally during the Rupelian (33.6–28.4 Ma) in a broadly WNW-ESE extensional regime (Bergerat, 1987; Villemin and Bergerat, 1987). The ECORS deep seismic profile (60 km north of the Dannemarie basin) images an east-dipping crustal-scale normal shear zone below the URG (Brun et al., 1992). The rift records a stretching factor (beta) of approximately 1.1–1.2 (Villemin et al., 1986; Brun et al., 1992), representing a horizontal extension of between 4 and 5 km (Hinskin et al., in press). While subsidence continued in the northern half of the graben into the middle Pliocene (3–4 Ma), a post-Chattian unconformity indicates uplift of the southern half of the URG, probably due to the arrival of the Alpine forebulge in the Miocene (Bourgeois et al., in press). The graben is bordered by two massifs cored by Variscan crystalline rocks, each with elevations of just under 1500 m. To the west, the Vosges massif lies in the footwall of the Vosges fault zone. To the east, the Black Forest massif lies in the footwall of the Rhine fault zone. Exhumation of the Vosges and Black Forest massifs can, in part, be regarded as rift shoulder uplift combined with footwall uplift across the basin bounding faults; however, stratigraphy and thermochronology studies record multiple uplift phases from the Late Cretaceous to Early Tertiary and from end Chattian to Pliocene (Bourgeois et al., 2004, in press; Ziegler and Dezes, 2005). Thus, these massifs experienced uplift before, during and after rifting.

The Dannemarie basin occupies the SW corner of the URG (Figs. 1 and 2). To the west, the basin is bordered by the southern termination of the Vosges fault zone, to the south by the Jura fold belt (that developed between 11 and 3 Ma), and to the east by the Mulhouse block, an eastward tilted fault block limited by the Illfurth fault zone. The Dannemarie basin measures approximately 20 km east to west and 50 km north to south (Figs. 1 and 2), and is filled by up to 1950 m of syn-rift sedimentary rocks unconformably overlain by Pliocene to Quaternary cover.

### 2.2. Stratigraphy and mechanical stratigraphy

Pre-rift stratigraphy of the southern URG comprises a Triassic to Upper Jurassic Tethyian passive margin succession of relatively constant thickness (1000–1200 m) overlying crystalline Variscan basement. Permo-Carboniferous clastics and volcanoclastics (>500 m) are preserved in local grabens oriented ENE-WSW (Schumacher, 2002; Ustaszewski et al., 2005), which are here treated as part of the competent Variscan basement. The detailed succession is represented in two boreholes (Fig. 3a), one from the centre of the Dannemarie basin (Bellemagny 1, used to define seismic stratigraphy), and the second from the Mulhouse fault block (Knoeringue). The Triassic succession comprises from bottom to top: (1) 120 m of coarse Bundstandstein fluvial clastics (seen in the Knoeringue borehole); (2) a mixed Muschelkalk succession of dolomites, limestones, clastics and evaporites (>230 m); and (3) Keuper evaporites, shales and dolomites (170 m). The 700–800 m thick Jurassic succession includes a marl-dominated Lias sequence (80–200 m), a limestone-dominated Dogger sequence (200–400 m) including the 130–170 m Grand Oolithe limestone, and the Malm succession comprises 200–400 m of limestones and shales (50:50). Therefore, in terms of mechanical stratigraphy, the pre-rift succession comprises a relatively competent unit of Dogger and Malm limestones, approximately 500 m thick, overlying an incompetent unit, 500–>800 m thick, of Lower Dogger, Lias and Trias evaporites, marls and shales (Fig. 3a).

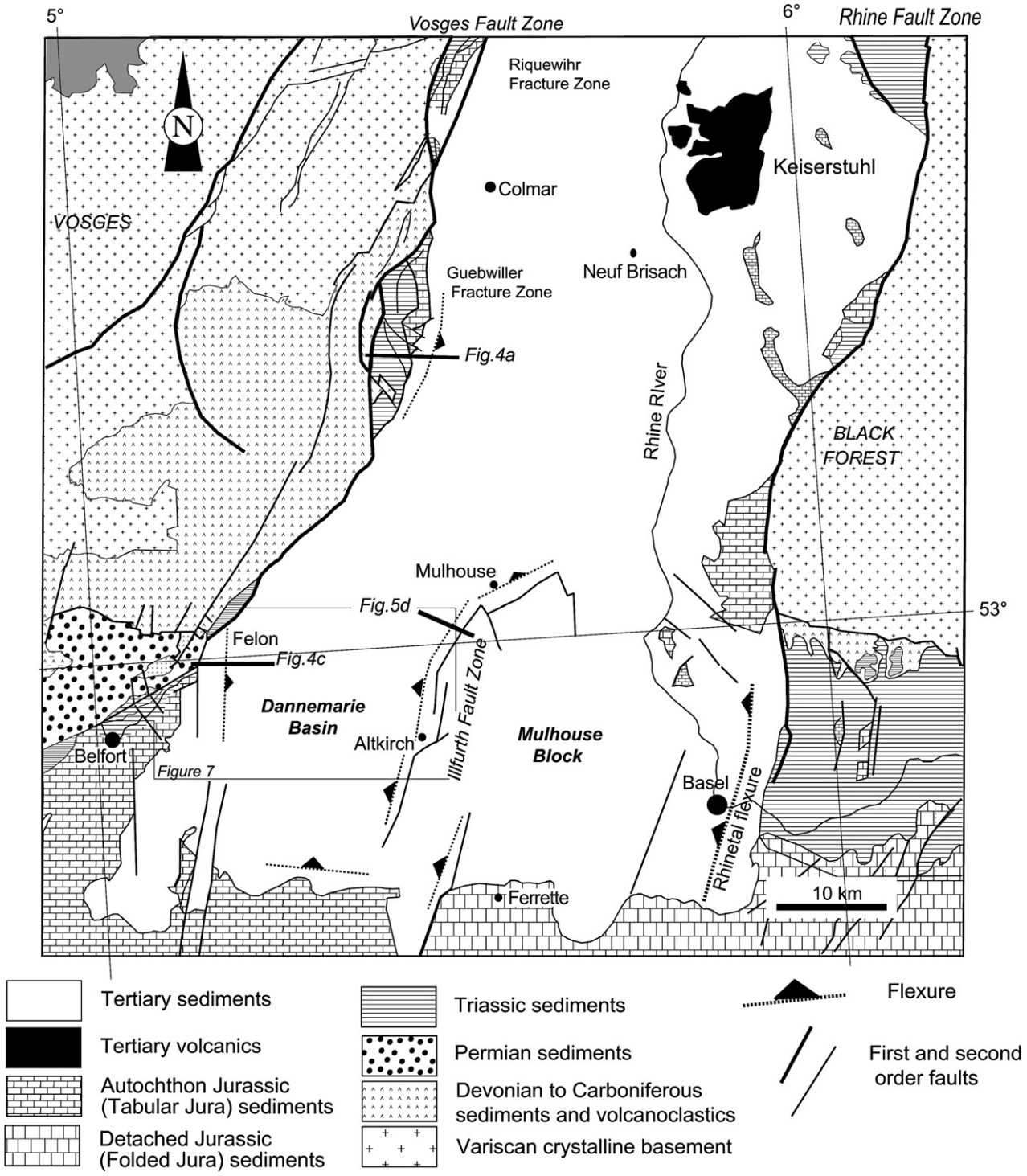


Fig. 1. Geological map of the southern Upper Rhine Graben (without Quaternary cover), showing the Dannemarie basin and cross-sections, including the Guebwiller cross-section on the Vosges fault zone. Principal monoclines and faults are shown. VF is the Vosges fault, RF is the Riquewihr fault, and CF is the Colmar fault. Adapted from BRGM maps.

Duringer (1988); Sissingh (1998, 2003); Berger et al. (2005a,b) and Hinskin et al (in press) describe the Tertiary stratigraphy of the URG. Thin Lutetian lacustrine deposits (<50 m, 46–40 Ma) lie unconformably on karstified Upper Jurassic limestones. Based on the biostratigraphic review of Berger et al. (2005a), the uppermost Lutetian to Lower Rupelian Salt Series comprises lacustrine marls, thin limestones and gypsiferous marls subdivided into three formations: the Lower (LSF, approximately 42.5–33.5 Ma), Middle (MSF, 33.5–31.5 Ma) and Upper Salt Formations (USF, 31.5–30.5 Ma), with a total thickness of approximately 1300 m. There is, however, some uncertainty regarding the age of the base of the LSF, which is placed at 35 Ma in publications other than Berger et al. (2005a) and Hinskin et al (in press), implying

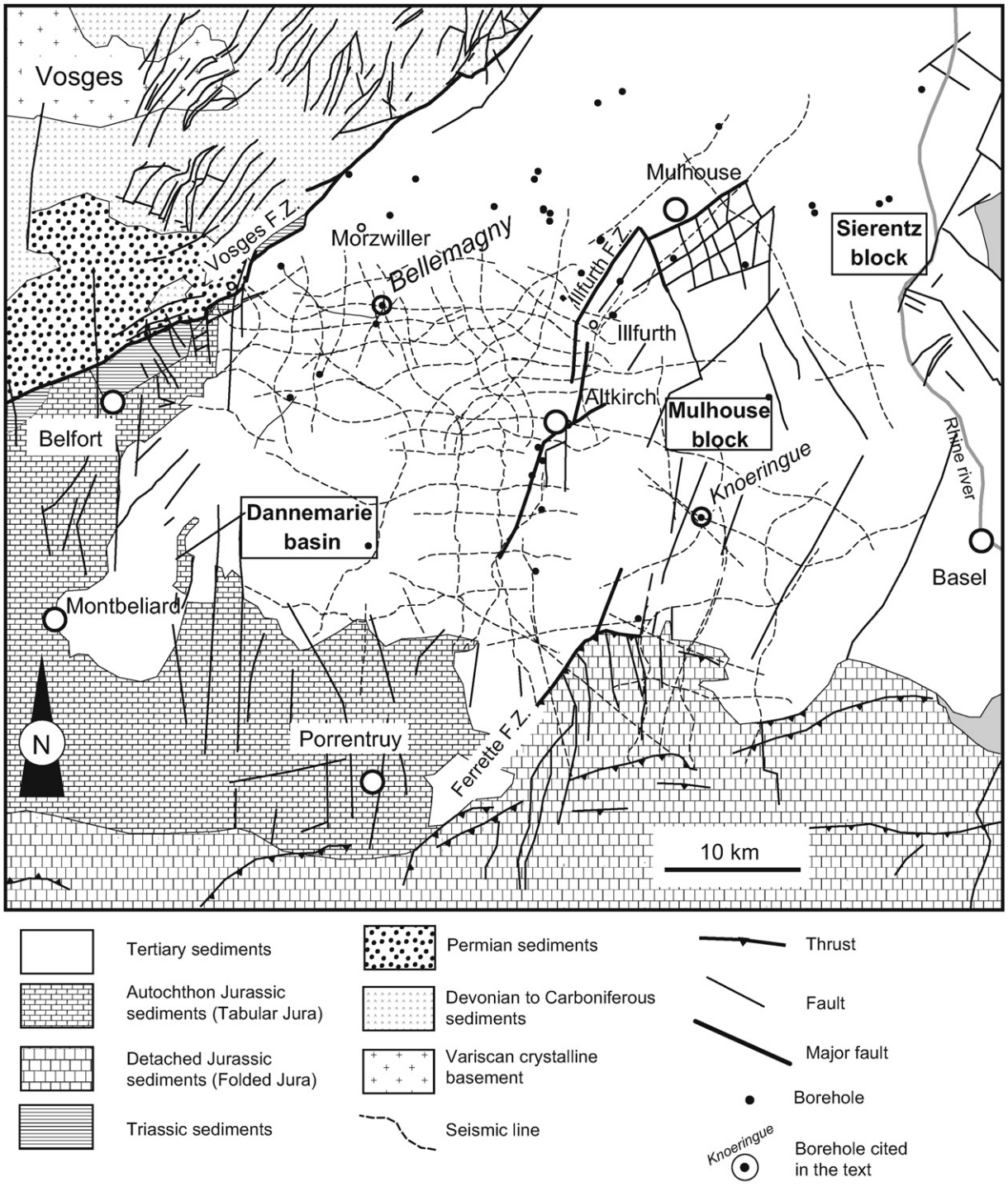


Fig. 2. Geological map of the Dannemarie basin (without Quaternary cover), showing all seismic lines and boreholes incorporated into the 3D gOcad model.

a significantly later onset of main subsidence. The Salt Series passes laterally into basin margin conglomerates and sandstones (''Conglomérats Côtiers'', Border Conglomerates) deposited in alluvial fans (Duringer, 1988; Hinskin et al., in press), reflecting pronounced syn-rift relief in both the Vosges and Black Forest massifs (but not on the Mulhouse block). These conglomerates show an inverse footwall stratigraphy, recording progressive unroofing of the footwall sequence (Theobald, 1977). In the late Rupelian to early Chattian, a shallow marine transgression led to the deposition of a marly sequence over a period of 2.5 Myr (30.5–28 Ma ''Série Grise'', Grey Series; <320 m). Chattian fluvial deposits (<350 m) are only locally preserved (Freshwater Molasse). These pass laterally into a thick succession of Gypsiferous Marls north of Mulhouse (Fig. 2). Miocene and Pliocene deposits are absent in the southern URG but occur in the

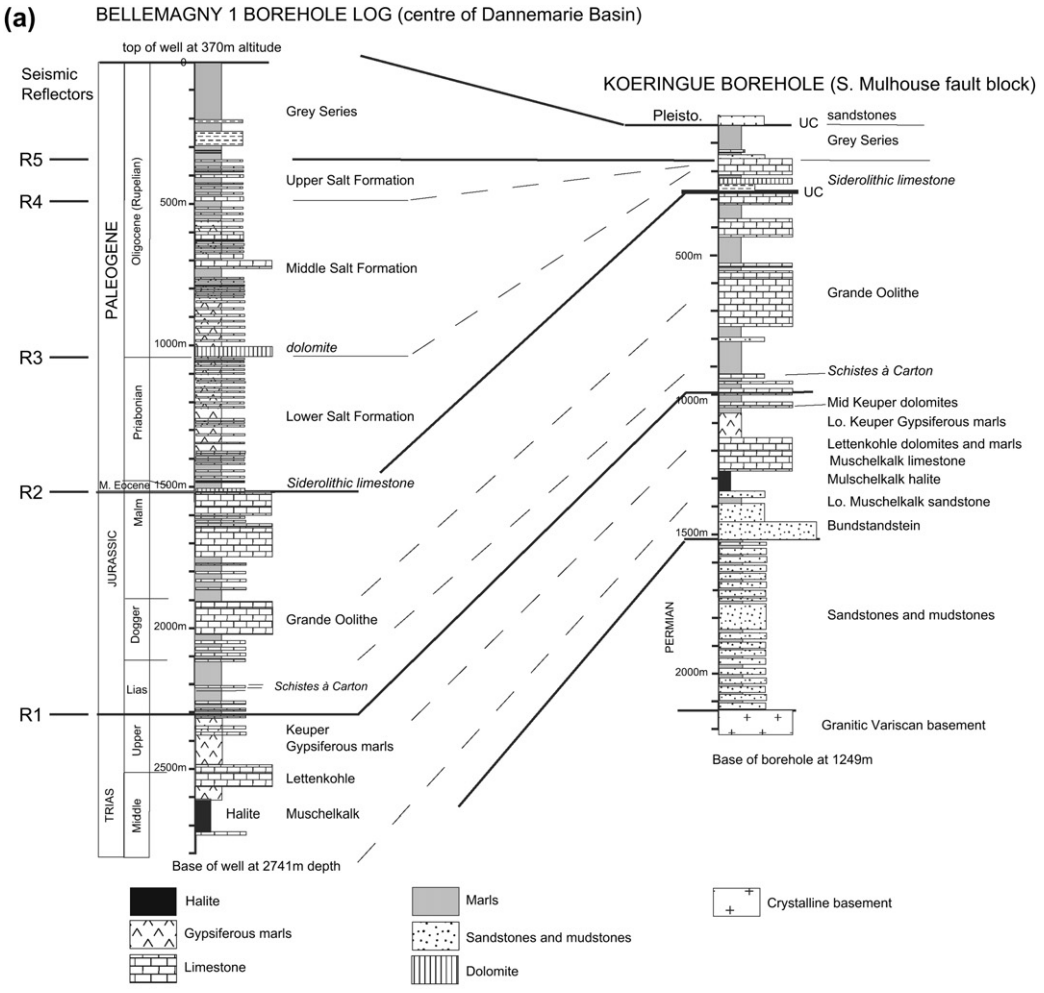


Fig. 3. (a) Synthetic logs of two boreholes, representing the stratigraphy of the Dannemarie basin (Bellemagny 1) and the Mulhouse fault block (Knoeringue), which are located on Fig. 2. The stratigraphic position of the principal reflectors identified on seismic lines, R1–R5, is shown. (b) Relationship between two-way time and depth, deduced for the Bellemagny 1 borehole and its intersecting and adjacent seismic lines. A 2nd-order polynomial, linking the depth (in m) to the two-way time (in s) was fitted to data by a least-squares method (see Le Carlier de Veslud et al., 2005 for details). This function has been used to migrate all seismic lines.

northern URG (<1500 m, Schumacher, 2002). Post-Chattian deposition is represented by the fluvial Sundgau Gravels of Pliocene age (<30 m, 2.9–4.2 Ma, Giamboni et al., 2004; Berger et al., 2005a).

Stratigraphic correlation (Fig. 3) shows that the Mulhouse block was not emergent during Tertiary rifting but accommodated deposition of a condensed succession of marls, gypsiferous marls and limestones equivalent to the Salt Series of the Dannemarie basin. The Grey Series and the Freshwater Molasse occur in both areas, but are only locally preserved so that their thicknesses are poorly constrained. In summary, the relatively incompetent Tertiary succession of the Dannemarie basin comprises up to 1950 m, whereas that of the Mulhouse fault block is less than 300 m.

### 2.3. Integration of data into a 3D geometrical model using gOcad

A 3D geometrical model of key stratigraphic horizons and faults was constructed using the gOcad geomodeling program (Mallet, 2002). The model incorporates the BRGM[1] well database and geological maps, 50 seismic sections and published stratigraphic studies. The gOcad 3D geomodeler represents a first-order tool for integrating different kinds of data and ensuring consistency between data and models. The 3D model clarifies lateral variations in basin-margin geometry and stratigraphic infill. Laterally changing fault-fold geometries are more easily studied in 3D space. Misinterpretation of geometries due to non-linear seismic profiles can also be avoided. However, this program was designed to build models using high density data sets, typically 3D seismic surveys. Therefore, the quality of the model is dependant on data density distribution and quality. Insufficient control or poor data can lead to invalid models. Construction of good quality models is a labour-intensive procedure requiring constant checks on quality and geological validity.

Enterprise Oil and Euromin shot seismic surveys across the Dannemarie basin and the Mulhouse block in 1987 and in 1985 respectively, using identical parameters and with an average line spacing of 1–3 km (Fig. 2). A geophone spread of 70 m–1350 m achieved a good velocity control from near surface to approximately 2000 m depth, imaging the Tertiary basin fill and the underlying Mesozoic sequence, and in places down to Triassic levels (Fig. 4). A 30 m station interval and a vibrator frequency band of 12–96 Hertz achieved high lateral and vertical resolution.

Correlation of the Bellemagny 1 borehole stratigraphy (2741 m depth, Fig. 3), situated in the centre of the basin, with adjacent seismic lines (details in Le Carlier de Veslud et al., 2005) established the seismic stratigraphy in two-way time (TWT). A 1D time-depth conversion law established for this borehole allows five stratigraphic markers to be correlated with seismic reflectors. These reflectors represent the base of the Jurassic succession (R1; not the base of competent Jurassic beds); the base of the Tertiary succession (R2); the base of the Middle and Upper Salt Formations (R3 and R4 respectively) and finally, the base of the Grey Series (R5). Locally, a sixth reflector is identified as the base of the Freshwater Molasse. A close similarity between velocities calculated at Bellemagny 1 and those calculated elsewhere in the basin using interval velocities on seismic lines, indicates that little or no lithological variation exists across the basin centre (Fig. 3b). We digitized stratigraphic reflectors and faults in gOcad and then performed a migration to depth using a time to depth conversion law derived from the Bellemagny 1 borehole (Fig. 3b). We then compared reflector depths to well data incorporated into the gOcad database and corrected them accordingly. Finally, we calculated and smoothed thickness maps of the different Salt Formations in 3D. It was not possible to compute a thickness map of the laterally equivalent condensed succession on the Mulhouse block.

### 2.4. The Vosges fault zone

The Vosges fault zone of the southern URG is over 150 km long (from Saverne to Belfort), separating the Upper Rhine Graben from the Vosges massif to the west. From Strasbourg to Guebwiller, the fault zone is oriented N10°E, turning to N30°E between Guebwiller and Belfort (Fig. 1). Analyses of fault kinematic data (Ustaszewski et al., 2005) indicate an overall E-W extension direction across the Vosges fault. Throw across the fault zone, the sum of hangingwall subsidence and footwall uplift, can be over 4000 m. In this paper, we analyse only hangingwall throw recorded in URG Tertiary stratigraphy, which decreases southward from 2900 m in the Guebwiller area (Mulhouse potash basin) to 1700–1500 m in the northern Dannemarie basin, 50 km to the south. From here, the syn-rift succession continues to thin southward along the western margin of the Dannemarie basin, as throw on the Vosges fault zone dies out. Along the southern margin, the basin fill wedges out across a broad E-W flexure (Ustaszewski et al., 2005). Here, we analyse the folds associated with the Vosges fault zone in the Guebwiller area and near its southern termination in the northern Dannemarie basin.

#### 2.4.1. Guebwiller area

The eastern part of the E-W cross-section in Fig. 4a is based on a seismic line recorded several kilometres SW of the town of Colmar by Clyde Petroleum for ESSO. Although the exact location of the seismic line is confidential, it lies just east of the Guebwiller faulted panel, a lozenge-shaped panel (<8 km wide) of sub-horizontal Liassic and Triassic strata (400 m thick) in small tilted blocks (Fig. 1), which lies between the Colmar fault and the Vosges fault to the west. Several authors have described and interpreted the stratigraphic geometries in the hangingwall of the Colmar fault zone imaged on this line in two-way time (Duringer, 1988; Maurin, 1995; Maurin and Nivière, 2000). Here, the line has been migrated using the same parameters as for the other seismic lines in this study. After migration, the syn-rift succession on the Guebwiller seismic line measures 2500–2900 m.

[1] BRGM, Bureau de Recherches Géologiques et Minières, the French national geological survey.

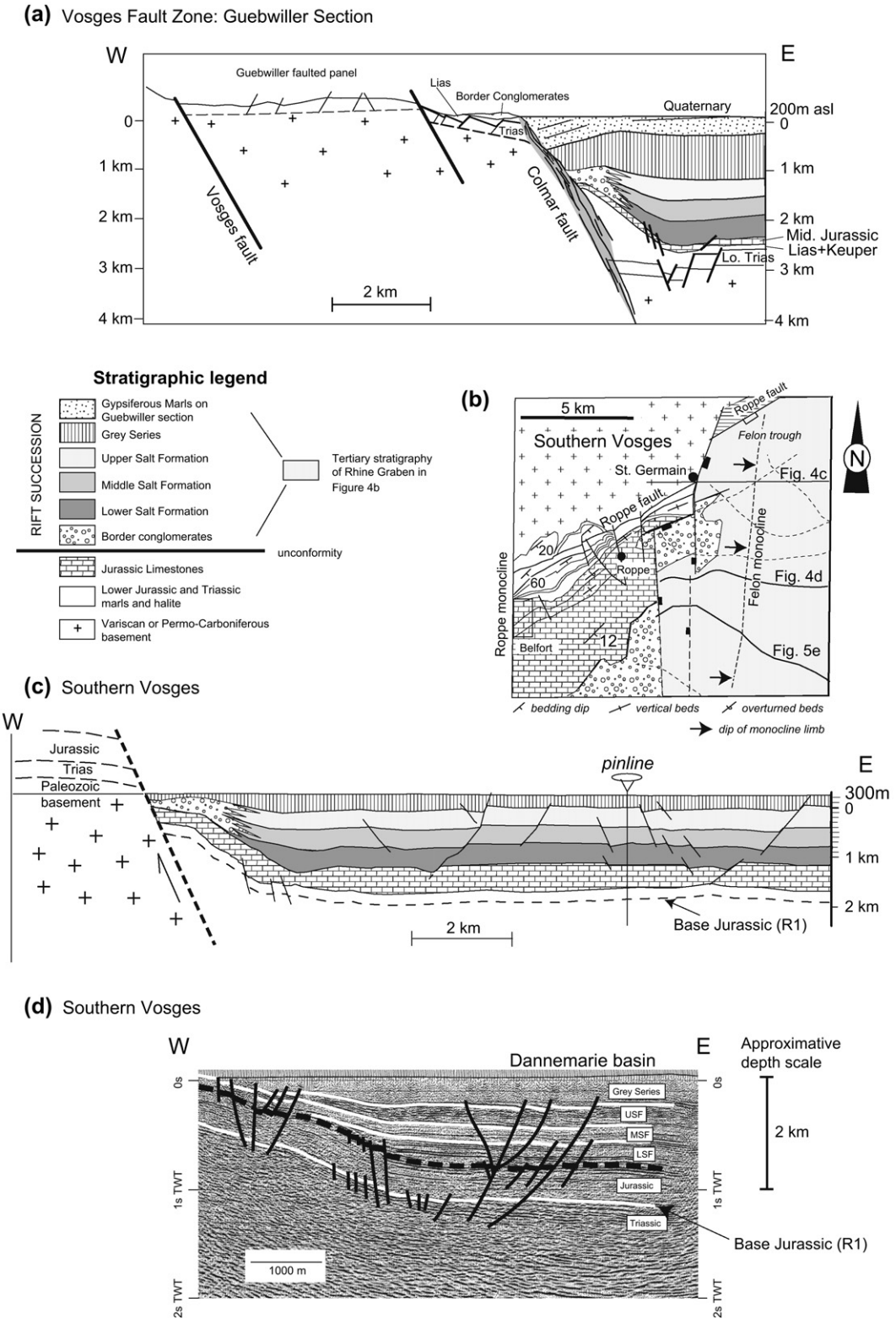


Fig. 4. Cross-sections across the Vosges fault zone. (a) Cross-section across the Guebwiller panel and the Colmar fault and monocline (approximately located on Fig. 1). (b) Geological map of the southern termination of the Vosges fault zone (located on Fig. 1). The positions of profiles c and d are indicated, as well as the western extremity of the seismic line in Fig. 5e. (c) W-E structural cross-section compiled from 3 seismic lines and geological maps. (d) W-E seismic cross-section through the Felon monocline. The cross-sections in a and c are sequentially restored and modelled using a trishear fold behaviour (Figs. 9 and 10).

Tertiary reflectors are identified by correlation with the seismic stratigraphy established in the Dannemarie basin. Reflectors and unit thicknesses correspond well with those of Lutz and Cleintuar (1999) on seismic profiles in the adjacent Mulhouse potash basin. Maurin and Nivière (2000) divide the syn-rift succession, without explanation, into Priabonian (equivalent to the LSF) and Rupelian (equivalent to the MSF, USF, GS and FM) units. Their resulting stratigraphic thicknesses do not correspond to those in surrounding areas (Lutz and Cleintuar, 1999). While we largely agree with their overall geometric interpretation, we propose a new stratigraphic correlation, which is more coherent with published Tertiary stratigraphy.

Using BRGM geological maps, the cross-section is extended to the west across the Guebwiller faulted panel (Fig. 1). On the eastern rim of this zone, Mesozoic strata dip eastward and are unconformably overlain by the Tertiary Border Conglomerates. The absence of the Malm succession and the thinness of the Grande Oolithe suggest a pre-Priabonian erosion of at least 500 m in this area.

The seismic section shows different fold geometries affecting the different syn-rift stratigraphic levels. A large monocline, involving strata from Keuper units to the Grey Series, is cut by a planar normal fault, here called the Colmar fault, that dips 70° east and cuts basement (Fig. 4a). In the hangingwall, Liassic marls and Keuper evaporites thicken against the fault, whereas the underlying Lower Triassic units appear to be faulted but not folded. The Salt Series thins rapidly from 1270 m to 250 m across the 45° monoclinal limb (2.5 km wide). These strata constrain growth of the monocline to syn-early rift. The Grey Series has a thickness of around 900 m, thinning slightly toward the fault. In contrast, the uppermost Gypsiferous Marls (equivalent to the Freshwater Molasse) are affected by a rollover anticline, thickening toward the fault from 400 m to 900 m. It is not possible to say whether this thickness change is due to late folding and erosion or due to syn-sedimentary anticlinal growth.

The hinge and the upper limb of the monocline are preserved in the footwall of the Colmar fault (Fig. 4a). This sub-horizontal, faulted panel terminates to the west against the Vosges fault, which records a minimum throw of 1000 m. Sub-horizontal bedding across the Guebwiller panel indicates that no tilting was associated with displacement on either the Vosges or Colmar faults.

#### 2.4.2. Western border of the Dannemarie basin

Southward from Saint Germain to Belfort (Fig. 1), the Vosges fault zone splits into two main branches oriented N-S (Felon) and NE-SW (Roppe), each associated with a major monocline. Displacement on these two branches and their monoclines dies out southward.

The Felon monocline has no surface expression but is imaged on eight seismic lines (Le Carlier de Veslud et al., 2005). The Salt Series thickens and dips eastward across the monocline (Fig. 5d,e). Seismic lines and the derived 3D model (Figs. 4, 6 and 7) show Tertiary units thinning southward as the amplitude of the monocline diminishes and the base of the Tertiary shallows. The thickest Tertiary stratigraphy is found at the northern extremity of this monocline in the Felon trough (Fig. 4; Le Carlier de Veslud et al., 2005) before it is truncated abruptly against the NE-SW Roppe fault. The monocline limb is cut by minor faults, dipping both east and west, that die out southward (Fig. 4). On the sub-horizontal upper limb of the monocline a small N-S graben cuts Tertiary strata.

The NE-SW Roppe fault is associated with a monocline that consists of a corridor of vertical to overturned Mesozoic beds separating gently SE-dipping Triassic sediments to the NW from a panel of Mesozoic and Tertiary sediments dipping gently SE (Fig. 4b; Theobald and Devantoy, 1963). This monocline and its fault zone die out to the SW of Belfort. To the NE, it terminates abruptly against a NS normal fault at Saint Germain. No Tertiary deposits are preserved across this fold and it is, therefore, not analysed in this paper.

### 2.5. Eastern border: the Illfurth fault zone

The Illfurth fault zone separates the Dannemarie basin from the Mulhouse block. It trends NNE-SSW in the south curving to NE-SW further north (Fig. 5a). Eight seismic lines show Jurassic strata defining a monocline tilted to the west in the fault's hangingwall (Fig. 5, Le Carlier de Veslud et al., 2005). Total vertical displacement of the Tertiary unconformity across the fault zone and its monocline reaches over 2000 m. Maximum throw on the fault segments alone, calculated using base Tertiary, reaches 900 m decreasing to the NE and SW (Fig. 6). The 30-km long fault zone comprises four segments (each 6–10 km long) that cut the present ground surface. The fault dies out NE of Mulhouse, where a monocline continues to accommodate substantial subsidence (Fig. 5d). Southwest of Altkirch, the fault tips out and the monocline amplitude decreases as it merges with the southern margin of the basin (Fig. 6a).

Across the Illfurth monocline, the Salt Series dips and thickens rapidly westward. Isopach maps of the three Salt formations (Fig. 7) show culminations and depressions along the synclinal and anticlinal axes of the monocline. While thickness variations in the Grey Series and the Freshwater Molasse are difficult to detect, both units dip west in the Illfurth monocline (Fig. 5c,e), suggesting that some tilting occurred during, or more probably after, the Chattian.

### 2.6. 3D basin model

An altitude map (above sea level) for the base Tertiary (Fig. 7a) is derived from the 3D gOcad model and shows the principal faults and flexures that controlled subsidence in the Dannemarie basin. The present day topographic surface is on average at 350 m above sea level, so that 1750 m of Tertiary infill are preserved at the north-western edge of the basin (Felon trough) and at the north-eastern side of the basin. Further south, the basin takes on a more asymmetrical form with all strata dipping east into the Hagenbach trough where 1950 m of Tertiary strata are preserved. The centre of the basin is affected only by minor normal faults trending NNE-SSW

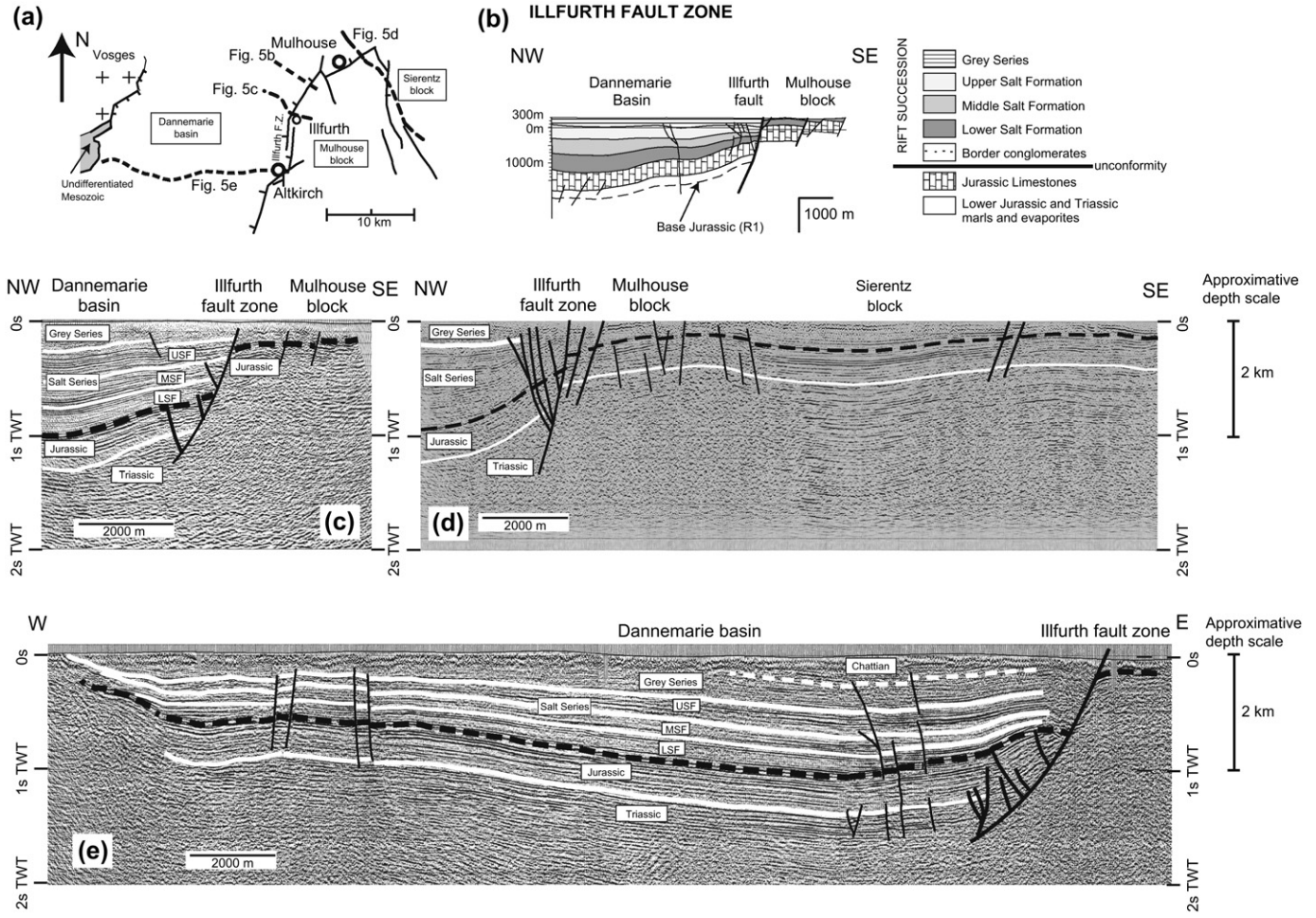


Fig. 5. The Illfurth fault zone. (a) Simplified map of the Illfurth fault zone showing the location of the structural cross-section in (b) and the three seismic lines in (c), (d) and (e). The cross-section in (b) is used for sequential restoration and trishear modelling (Fig. 11).

with throws of less than 100 m (Figs. 4d and 5e). The Jurassic is of constant thickness (~700 m) across the whole area.

The thickness map of the LSF shows a 15-km long depocenter, trending NW-SE from Felon to Carspach with a maximum thickness of over 550 m in the Felon trough (Fig. 7b). The LSF basin closed gently toward the south and southwest. To the west the N-S Felon monocline controlled the basin margin and terminates abruptly against the Roppe fault (Fig. 4b). This suggests that the Roppe fault is a younger structure. The Illfurth monocline controlled the eastern basin margin. A major culmination is clearly visible along the anticlinal axis. On the Mulhouse block 230–80 m of equivalent strata were deposited during this period (42.5–33.5 Ma).

The MSF, deposited during the period from 34 Ma to 32.5 Ma, has a maximum thickness of 500 m (Fig. 7c) and displays roughly the same pattern as the LSF, thickening northward into the Mulhouse basin. However, the NW-SE depocentre trend is less evident as subsidence was controlled principally by the Illfurth and Felon monoclines. Fifty to thirty metres of equivalent strata were deposited on the Mulhouse block.

The USF map (Fig. 7d), indicates a maximum thickness of ca. 500 m in the Felon trough. While the Felon trough continued to dominate the western basin margin, a major N-S depocentre (>400 m) ran parallel to the Illfurth fault zone (for 10 km) passing northward into the Mulhouse basin. The associated Illfurth monocline was narrower and longer. On the Mulhouse block, around 100 m of equivalent strata were deposited.

Thickness variations in the Grey Series are less well constrained. However, its reflectors remain parallel, and are cut either by the erosion surface or by the Illfurth fault zone. Seismic and borehole data indicate a similar thickness of Grey Series in the Dannemarie basin and on the Mulhouse block. This implies that the Illfurth fault was inactive during deposition of a constant thickness of Grey Series and Freshwater Molasse across the area. Post-Chattian reactivation of the Illfurth fault led to uplift and erosion of the western part of the Mulhouse block.

## 3. Trishear modelling

Using Tertiary growth strata, the sequential restoration of each of the three cross-sections presented above (Figs. 4 and 5) provides: (1) a simplified sequence of fault activation; (2) progressive displacement along each fault; and (3) the thickness and geometry of growth strata for any given period. These

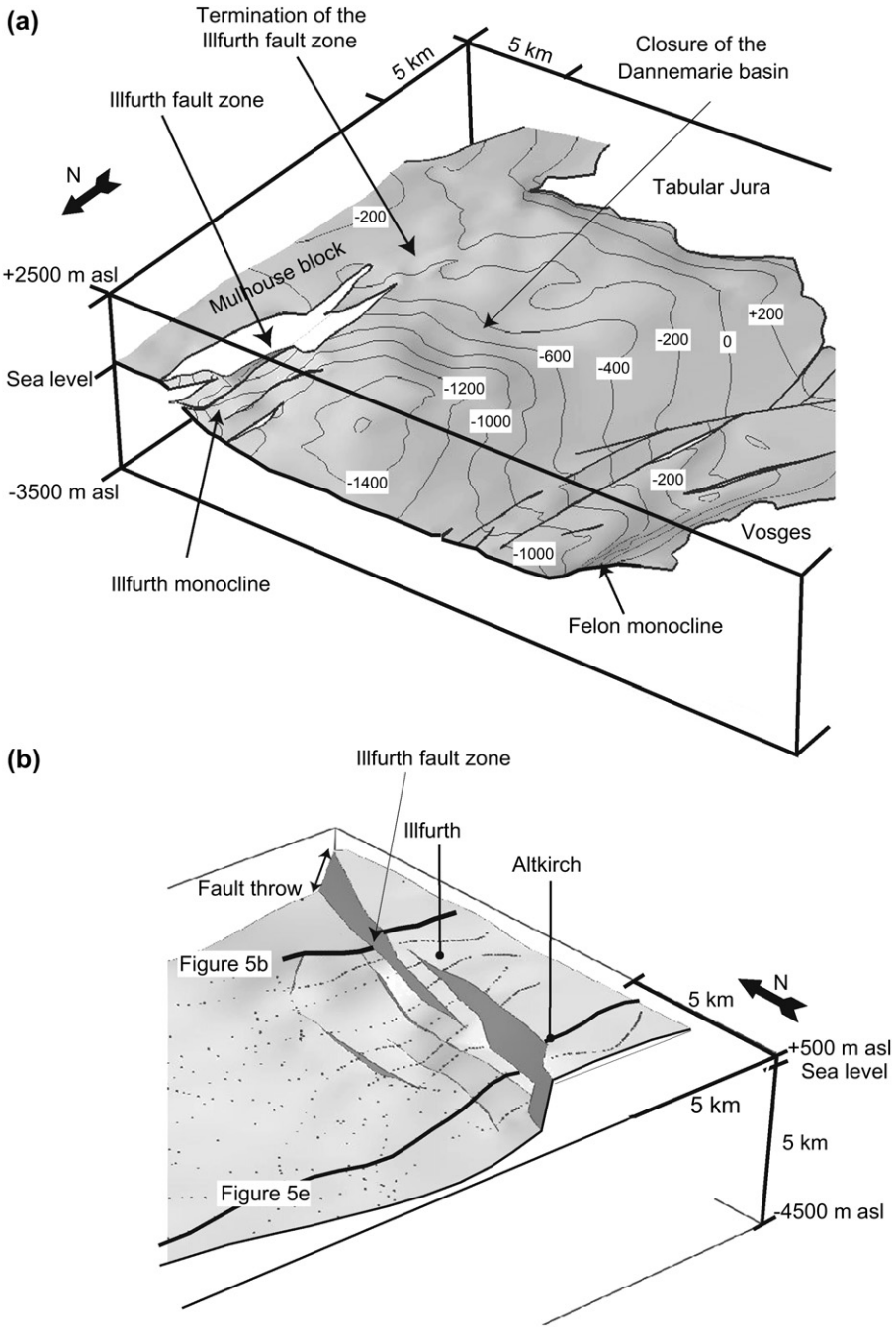


Fig. 6. 3D images of the Dannemarie basin derived from the gOcad model. The base Tertiary unconformity is shown in shaded relief. (a) View toward the SE from the Vosges massif toward the Illfurth fault zone and the Mulhouse block (vertical exaggeration is 1.5). (b) View toward the NE toward the Illfurth fault zone. Fault surfaces are shown in dark grey. Dots on the surface are data points for base Tertiary from seismic lines and boreholes. No vertical exaggeration.

results are used to constrain forward kinematic models of fault-propagation folding using the FaultFold software (Allmendinger, 1998; Zehnder and Allmendinger, 2000, see website http://www.geo.cornell.edu/RWA/trishear/default.html). The purpose of this software is to numerically simulate the trishear kinematic model that was initially proposed by Erslev (1991) and developed by Hardy and Ford (1997); Allmendinger (1998); Hardy and McClay (1999) and Zehnder and Allmendinger (2000). In this model, the fold is generated within a triangular shear zone that opens upward from the fault tip (Fig. 8). Both the fault and its associated triangular shear zone migrate upward through a given stratigraphy; thus replicating fault tip and ductile bead migration. This approach is purely kinematic and geometric with no mechanical properties assigned to stratigraphy. The controlling parameters in a trishear model are (Fig. 8): (1) the initial location of the fault tip; (2) the dip of the fault; (3) the displacement (slip) along the fault, S; (4) the aperture angle of the triangular shear zone (trishear angle); and (5) the P/S ratio, where P is fault-tip propagation rate (Allmendinger et al., 2004). Syn-sedimentary fold

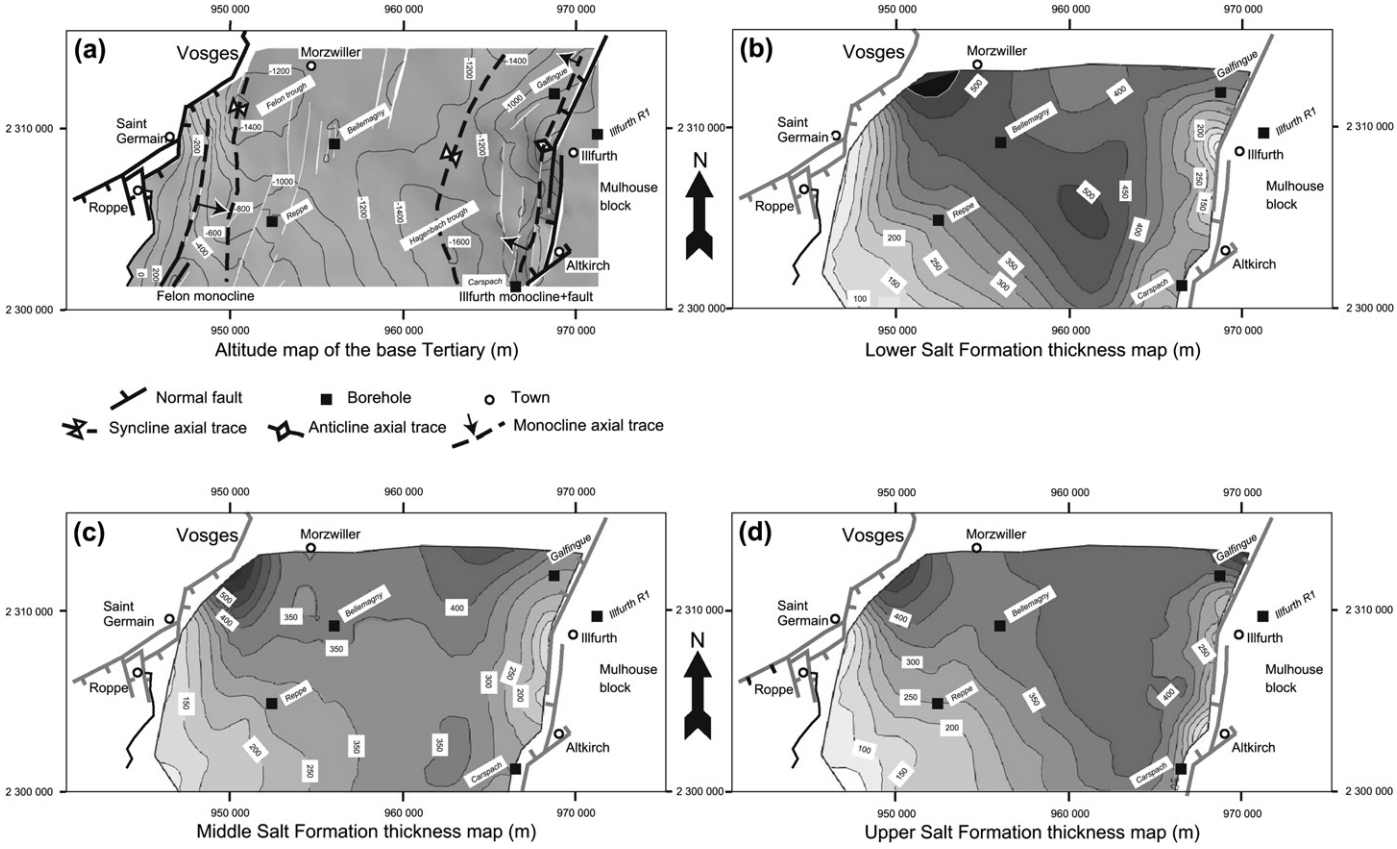


Fig. 7. (a) Altitude map (above sea level) of the base Tertiary (extended Lambert II coordinate system) in the Dannemarie basin. The altitude of the present day topographic surface is around 350 m above sea level across the whole basin. The gaps in the base Tertiary surface correspond to heave on normal faults. The axial traces of syn-rift monoclines, anticlines and synclines are shown. Scale notches are spaced at 10 km. (b)–(d) Isopach maps of the Lower, Middle and Upper Salt Formations derived from the gOcad model. Present-day fault traces are shown in grey. Equivalent but thinner units were deposited on the Mulhouse block but they cannot be represented due to lack of control data.

geometries can be reproduced by the progressive addition of growth strata during a model run, assuming a simple horizontal percentage fill.

For modelling purposes, the pre-rift stratigraphy of the three cross-sections was simplified to three units comprising basement (Variscan crystalline basement and local Permian sediments), 800 m of Lower Jurassic and Triassic (incompetent) marls, shales and evaporites, and 500 m of Middle to Upper Jurassic (competent) limestones (200 m for the Guebwiller section). Available seismic data were not accurate enough to define the exact position or geometry of controlling faults at depth. However, the monoclines described above correspond to gravimetric discontinuities attributed to Variscan and Permian structures by Edel et al. (2002, 2007). We, therefore, assume that monoclines developed above reactivated basement faults and that the initial fault tip was located at the base of the Triassic succession. Fault kinematic data (Ustaszewski et al., 2005) indicate that extension was orthogonal to the modelled cross-sections.

About 20 forward models were tested for each of the three cross sections varying the fault dip (50–80°), the trishear angle and the P/S ratio (negative for normal faults), but also tuning other parameters. A set of 'best fit' common parameters was thus defined. All modelled faults dip at 70°. The most appropriate trishear angle was found to be 120°. Observed geometries suggest that there is more hangingwall area involved in deformation than footwall area. This is best replicated by a trishear angle asymmetry of 60% in the hangingwall. Fold restoration suggests that more than one fault controlled flexures at any one time. However, the trishear model does not allow for more than one fault to be active at any one time. Therefore, faults were activated sequentially or alternately in model runs.

### *3.1. Western border of the Dannemarie basin (Fig. 9 and Table 1a)*

Sequential restoration of the cross-section in Fig. 9a shows that the Felon monocline developed principally during deposition of the Salt Series. Basinward dips of the Grey Series record later tilting. Maximum thickness of the observed Tertiary succession on this cross-section is 1550 m, however, this excludes the Freshwater Molasse, which is not preserved.

The LSF (400 m max.) and MSF (350 m max.) onlapped a gentle monocline over 4 km wide (Fig. 9b). Their geometries were reproduced in the FaultFold program using displacements of 600 m (LSF) and then 350 m (MSF) on the F1 fault with a P/S ratio of 0 (Fig. 9c). The geometry of the USF strata

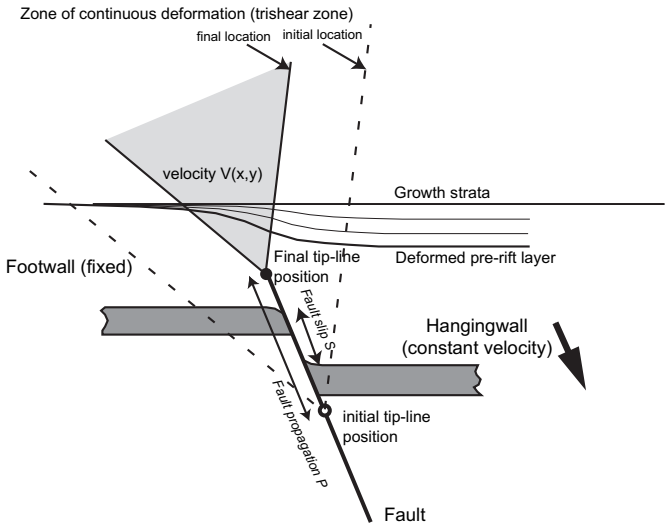


Fig. 8. Schematic diagram illustrating the parameters needed to model an extensional fault-propagation fold in trishear using the FaultFold software. Adapted from Allmendinger (1998).

(400 m; showing little flexure and mainly fault control) was replicated in FaultFold by transferring displacement onto a new fault, F2, located 1.5 km west of F1. Displacement on F2 was 500 m and the P/S ratio was −3 (Fig. 9c). The Grey Series (400 m) does not show syn-sedimentary wedging, as attested by its parallel internal reflectors. Its deposition was reproduced by a displacement of 450 m on the F2 fault (Fig. 9b,c). The F1 fault may have been active throughout F2 activity but this cannot be reproduced in the FaultFold software. Deposition of the Freshwater Molasse and later tilting and displacement on the F2 fault were not modelled.

In summary, total accommodation space created across the Felon monocline and its faults is 1550 m. Deposition of the LSF and MSF (750 m) was accommodated principally by a monoclinal flexure with faulting (on F2) taking over during deposition of the USF (400 m). Deposition of the Grey Series (400 m) was accommodated principally on the F2 fault. Therefore, the flexure created approximately 48% of accommodation space (un-decompacted) on this section line.

### 3.2. Colmar fault in the Guebwiller area (Fig. 10 and Table 1b)

In the Guebwiller cross section the thickness of the competent Jurassic limestone is 200 m. In this model, the accommodation space for the LSF (Fig. 10b) was progressively created by a gentle monocline with an eastward dip of 8° over 4 km. In FaultFold, this flexure was generated above the fault F3 with slip of 550 m and a P/S ratio of 0. During deposition of the MSF, the monocline broadened to over 5 km with a tilt of 15°E (on top Jurassic; Fig. 10c). This geometry was replicated in FaultFold by transferring displacement onto a new fault (F4) located 1.5 km west of F3 with a slip of 400 m (P/S = 0). During deposition of the USF, the flexure widened again to over 6 km and its eastern section steepened to 40°E (slip on F4 = 500 m, P/S = 0; Fig. 10c). The Colmar fault (F4) breached the monocline (Fig. 10b,c) during deposition of the Grey Series (900 m), which was partially controlled by flexure but principally by the planar Colmar fault. Its geometry is replicated by a 1200 m slip along F4, with a P/S of −3. During the Chattian, Gypsiferous Marls were deposited against the emergent Colmar fault, which can be modelled in FaultFold with an 800 m slip along F4 with a P/S of −1. Finally, a post-depositional rollover anticline which, following Maurin and Nivière (2000), was modelled as developing above a listric fault (D in Fig. 10c) rooted into a Liassic décollement (Fig. 10a,c).

In summary, total accommodation space created across the Colmar fault and its flexure is over 3000 m with three components from bottom to top: (1) 1250 m on the monocline alone (Salt Series); (2) 1550 m mainly on a planar fault (Grey Series and Gypsiferous Marls); and finally, (3) several hundred metres (unconstrained) on a late listric fault. The monocline thus created all accommodation space during early rifting, which represents approximately 42% of total accommodation space (un-decompacted).

### 3.3. The Illfurth fault zone (Fig. 11 and Table 1c)

During the Late Priabonian to Early Rupelian, a broad (5–6 km) gentle monocline accommodated deposition of the LSF and MSF (Fig. 11). This monocline can be reproduced in FaultFold using fault F5 with a displacement of 450 m (LSF) and 400 m (MSF), associated with a P/S ratio of 0 (Fig. 11c). The USF (350 m) was accommodated by a significantly narrower flexure (about 1.5 km). In the FaultFold model, displacement was transferred onto a new fault, F6, located 2 km eastward with a higher P/S ratio to −1, which forced the fault to propagate up into the Jurassic strata without breaching completely. This sequence allows deposition of 1270 m of Salt Series in the Dannemarie basin and approximately 250 m on the upper limb of the monocline, now the Mulhouse block (Table 1c).

While thickness estimates of the Grey Series are relatively constant across the Illfurth Fault, thicknesses of the Freshwater Molasse are not well constrained. It was assumed that the fault zone was inactive during deposition of the Grey Series and the Freshwater Molasse (700 m). Present-day throw on the Illfurth fault is estimated at 450 m with another 150 m throw on a synthetic fault 1 km to the east (Fig. 11a). Therefore, a post-Chattian reactivation of the Illfurth fault zone with ca. 600 m throw is necessary to explain observed geometries. If a continuous Freshwater Molasse layer is assumed, late reactivation would have been associated with up to 800 m of erosion of the western Mulhouse block.

In summary, total vertical displacement across the Illfurth fault zone and its associated monocline on this section line is approximately 2000 m, 1270 m (63%) of which was accommodated by the monoclinal flexure alone during deposition of the Salt Series. We propose that the fault zone and its monocline were inactive during deposition of the Grey Series and

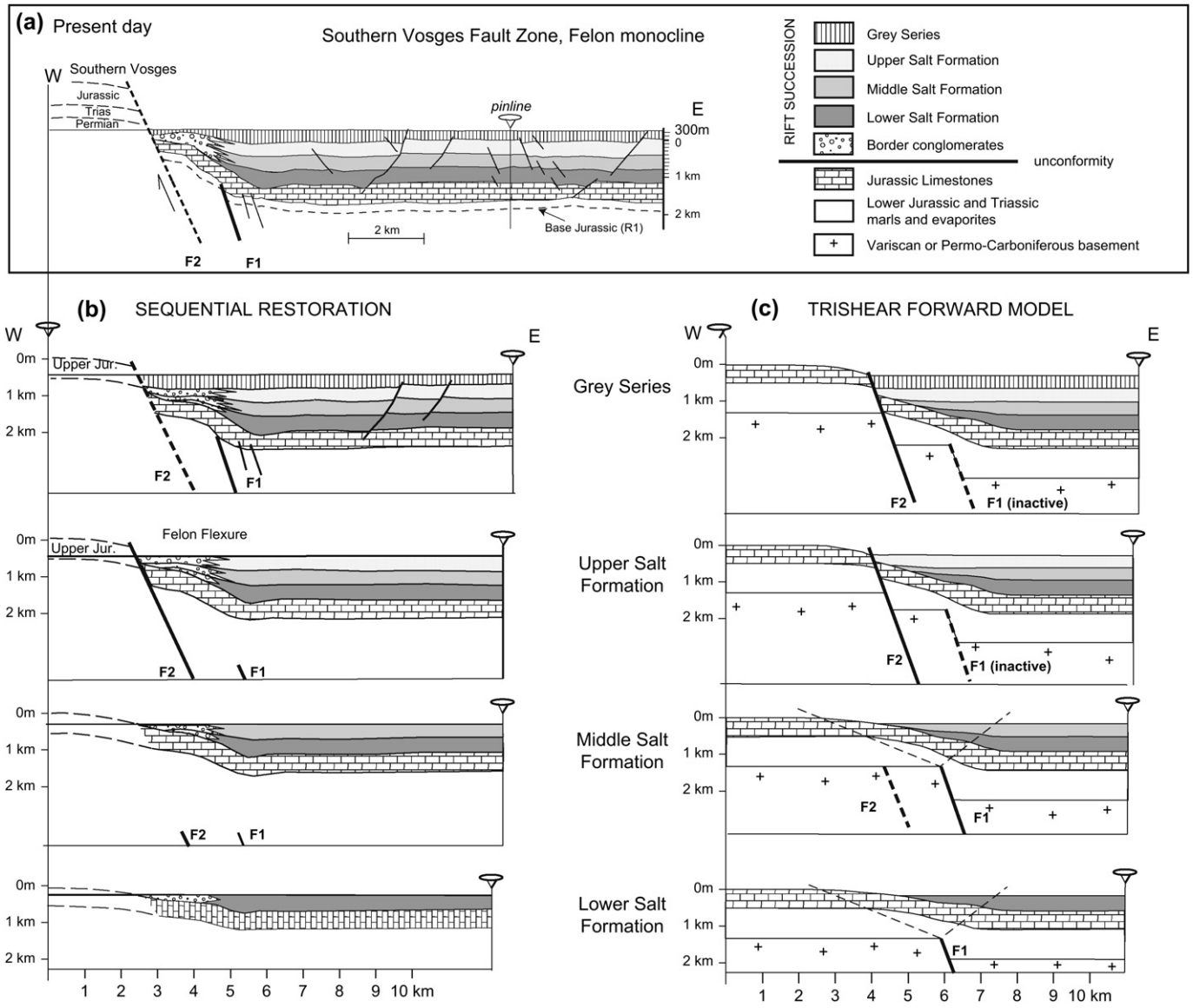


Fig. 9. (a) East-west cross-section across the southern termination of the Vosges fault showing the Felon monocline. Section located on Fig. 1. (b) Four-step sequential restoration of Tertiary strata. (c) Results of a forward trishear model of fault-propagation folding using the FaultFold software. Steps correspond to those in (b). Model parameters are shown in Table 1a.

Freshwater Molasse. Post-Chattian deformation was not modelled.

## 4. Discussion

### *4.1. Folding and faulting interaction during URG rifting*

We interpret the Dannemarie and Guebwiller monoclines as syn-sedimentary extensional fault-related folds for the following reasons: (1) the wedging of the Salt Series strata clearly dates folding as syn-rift; (2) folds coincide with and run parallel to principal normal faults and show typical hangingwall syncline geometries; and (3) fault-fold geometries can be reproduced as extensional fault-propagation folds by trishear kinematic modelling using reasonable parameter values. The above analyses show that, during the early stages of URG rifting (Salt Series), around 1300 m of accommodation space was created by flexure of Mesozoic strata on both margins of the Dannemarie basin and in the Guebwiller area further north. We estimate that these folds created 42–63% of the Tertiary accommodation space. While previous studies have concentrated on single structures, this work, along with that of Jackson et al. (2006) in the Suez rift, illustrates that fault-propagation folds can play a significant role in accommodating 3D regional extension during early rifting. These basin margin structures do not record lateral propagation but, rather, accommodated synchronous and equivalent subsidence along their lengths. Their location and orientation correspond to gravimetric discontinuities attributed to Variscan and Permian structures by Edel et al. (2002, 2007), suggesting that they developed above

Table 1
Parameters used in the trishear models presented in Figs. 9, 10 and 11

| Period | Slip along fault (m) | P/S | Max. thickness of sediments (m) | |
|---|---|---|---|---|
| **(a) Vosges, South section** | | | | |
| LSF (Priabonian) | F1: −600 | 0 | 400 m | |
| MSF (L. Rupelian) | F1: −350 | 0 | 350 | |
| USF (L. Rupelian) | F2: −500 | −3 | 400 | |
| Série Grise (U. Rupelian) | F2: −450 | −0.5* | 400 | |
| **(b) Vosges, Guebwiller section** | | | | |
| LSF (Priabonian) | F3: −550 | 0 | 450 | |
| MSF (L. Rupelian) | F4: −400 | 0 | 350 | |
| USF (L. Rupelian) | F4: −500 | 0 | 460 | |
| Série Grise (U. Rupelian) | F4: −1200 | −3 | 900 | |
| Chattian | F4: −800 | −1* | 650 | |
| Post-Chattian | D: −200 | | Rollover anticline | |
| **(c) Illfurth section** | | | | |
| | | | Dannemarie basin | Mulhouse block |
| LSF (Priabonian) | F5: −450 | 0 | 500 | 125 |
| MSF (L. Rupelian) | F5: −400 | 0 | 420 | 50 |
| USF (L. Rupelian) | F6: −350 | −1 | 350 | 50 |
| Série Grise (U. Rupelian) | No more activity | – | 350 | 350 |
| Chattian | No more activity | – | 350 | 350 |

Note that negative values of P/S combined with negative slip produce normal faults. *P/S ratio has no longer any significance because the fault tip is now above erosion level.

synchronously-reactivated basement faults. The Vosges fault zone dies out southward and is replaced by two extensional monoclines, one N-S (Felon) and the other NE-SW (Roppe), that in their turn, die out gradually to the south (Fig. 7a; Le Carlier de Veslud et al., 2005). The Roppe monocline and fault correspond to the location of a Late Palaeozoic basin margin fault as reconstructed by Ustaszewski et al. (2005). The isopach maps of the Salt formations show the gradual southward termination of the Felon monocline over 10 km. They also show the marked axial culmination in the centre of the Illfurth monocline corresponding to the point of maximum displacement on the fault zone. This axial culmination has a complex morphology associated with relay ramps along the Illfurth fault zone (Figs. 6 and 7).

Monocline amplitude and tilting of Mesozoic and Cenozoic strata in the Guebwiller area are higher than those in the Dannemarie basin. Maurin and Nivière (2000) report syn-rift fold limb dips up to 80° in the Riquewihr fracture zone further north (Fig. 1). The monocline was breached in the late Rupelian. From the late Rupelian to Chattian considerably higher subsidence was accommodated on the planar Colmar fault. This section shows that, in the presence of a weak detachment, a single fault zone can accommodate extension on an early fault-propagation fold, then on a planar fault that can finally evolve into a listric geometry by detaching on Liassic strata giving a rollover anticline.

In the Dannemarie basin, controlling faults began to cut up through their monoclines in the mid Rupelian time. Some component of folding may have continued after breaching. The 3D model of the Illfurth fault zone (Fig. 6) shows that the monocline is cut by a series of fault segments that are connected by breached or unbreached relay ramps. These segments probably propagated up from a common underlying master fault in the basement. Subsequent subsidence (late Rupelian to Chattian) was accommodated principally on the Vosges fault zone while the Illfurth fault zone became inactive. Several later phases of uplift during the Aquitanian, at the end of the Burdigalian and in the Plio-Quaternary (Giamboni et al., 2004) reactivated the Vosges and Illfurth faults, principally causing footwall uplift and erosion. These events are recorded by basin-ward tilting of the Grey Series and the Freshwater Molasse and by erosion of the Mulhouse and Vosges blocks.

Analogue and numerical modelling of extensional fault-propagation folds indicate that the deformation (heave) associated with extensional fold development can be accommodated either by extension in the proto-footwall and/or in the proto-hangingwall and/or by stretching of the tilted fold limb on a network of upwardly divergent secondary normal faults (Withjack et al., 1990; Withjack and Callaway, 2000; Finch et al., 2004; Jackson et al., 2006; Hardy and Finch, 2006). On the three analysed cross-sections, the estimated heave during deposition of the Salt Series is between 400 and 500 m, which must be accommodated somewhere in the section by extension of competent Mesozoic strata. All fold limbs show secondary normal faults. Extensive secondary faulting across the Mulhouse block (Fig. 2) suggests that significant strain was transferred into the proto-footwall of the Illfurth monocline (Fig. 5). A component of strain across the Felon monocline may be accommodated by a N-S graben imaged in its upper limb (Fig. 4). On the Guebwiller section, this strain may have generated tilted blocks across the Guebwiller panel in the footwall of the Colmar fault. Maurin and Nivière (2000) describe a similar panel of tilted blocks in the footwall of the Riquewihr fault further north, with all secondary faults rooting

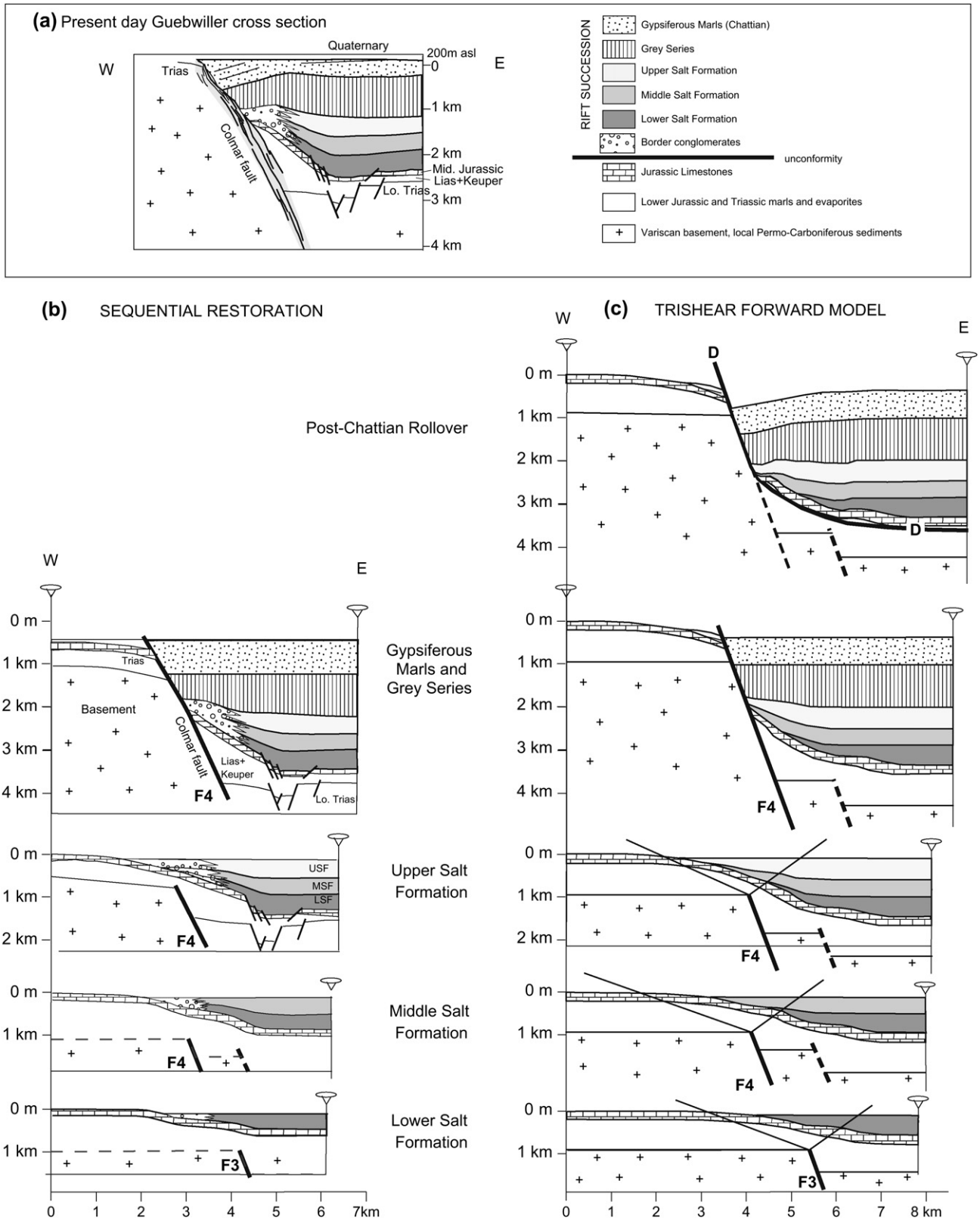


Fig. 10. (a) East-west cross-section across the Vosges fault zone in the Guebwiller region approximately located on Fig. 1. The Guebwiller panel is based on the BRGM Neuf-Brisach geological map (Theobald, 1977) passing through the villages of Pfaffenheim and Osenbach. The Triassic succession in the Guebwiller panel comprises 150 m Bundsandstein, 160 m Muschelkalk and several tens of metres of Keuper evaporites and marls. (b) Four-step sequential restoration of Tertiary strata. (c) Forward trishear model of the Guebwiller fault-propagation fold using the FaultFold software. Steps correspond to those in (b). In the model, the thickness of the competent Jurassic limestone is 200 m. Parameters used in this model are shown in Table 1b.

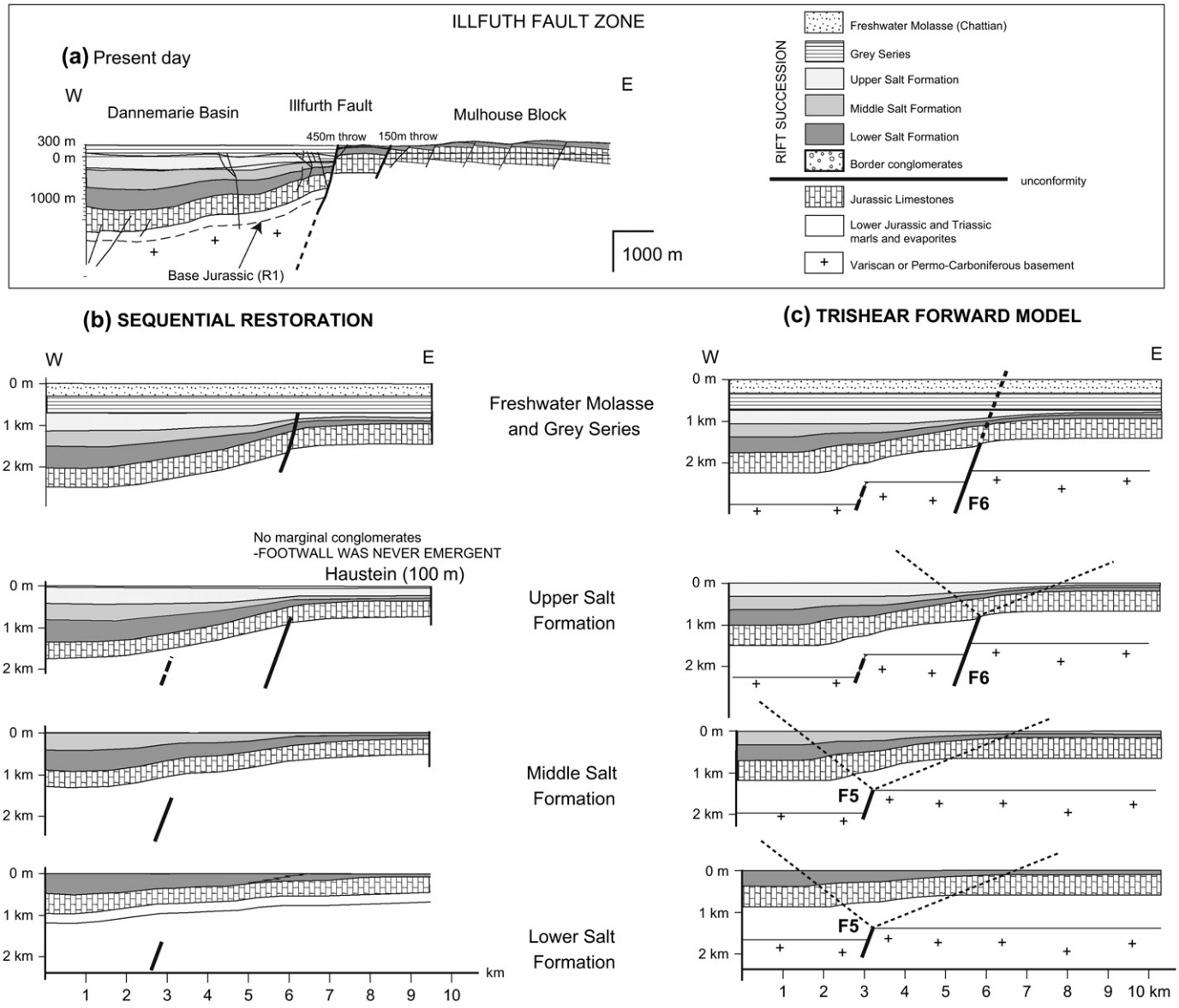


Fig. 11. (a) East-west cross-section across the Illfurth fault zone (located on Fig. 5). (b) Four-step sequential restoration of Tertiary strata. (c) Forward trishear model of the Illfurth fault-fold zone using the FaultFold software. Steps correspond to those in (b). Parameters used in this model are shown in Table 1c.

down into Keuper evaporites (Riquewihr panel, Fig. 1). The presence of this sub-horizontal footwall panel records the absence of footwall uplift across the Colmar fault, as the footwall block was not isostatically unloaded during early extension. The footwall uplift necessary for the creation of the Vosges mountains (and to supply the basin margin conglomerates) therefore occurred on the faults forming the western limits of these two lenticular horizontal panels (Fig. 4).

Rotstein et al. (2005a) argue that the Felon monocline developed as a late alpine transpressive fold in the footwall of a N-S thrust. As we have shown, the stratigraphic architecture of the Salt Series across this fold demonstrates its syn-rift origin and therefore a late transpressional origin can be ruled out. While a late sinistral reactivation of the Illfurth fault zone as proposed by Nivière and Winter (2000) and Giamboni et al. (2004) may have occured, syn-rift stratigraphic architecture demonstrates that the folds on the western and eastern limits of the Dannemarie basin are principally extensional in origin. Ustaszewski et al. (2005) propose a similar origin for the monocline that defines the southern closure of the basin.

The distribution of fault-related folds for the whole URG is not yet fully documented, nor is their evolution fully understood on a regional scale. We speculate that similar fold geometries imaged on seismic lines at the eastern margin of the southern URG may record some early syn-sedimentary extensional folding as well as the late transpressional event interpreted by Laubscher (2001) and Rotstein et al. (2005b). In contrast, seismic lines from the northern URG published in Derer et al. (2005) do not display any obvious syn-rift monoclinal geometries.

### 4.2. Controlling factors in the generation of URG fault-related folds

Why are extensional folds so widely developed in the southern URG? Due to their appropriate scaling parameters, the analogue models of Withjack and Callaway (2000) (1 cm = 100–1000 m) can be conveniently compared to the URG situation. Fig. 12 compares two seismic lines from the Dannemarie basin margins with analogue models of Withjack and Callaway (2000). Assuming 1 cm = 250 m, the 3–4 cm overburden layer in these models can correspond to the ca. 800–1000 m competent Jurassic succession of the URG (Fig. 12). The models also include a silicone layer representing the incompetent unit between basement and Jurassic limestones. Similarly, the 3–6 cm of syn-tectonic strata in the model appropriately represent the 500–2000 m of Tertiary deposits. Continuing with this correlation, we propose that the basin-controlling faults cut downward into basement and that the top of basement is sub-horizontal, requiring rapid lateral thickness changes in the viscous layer (largely in the Traissic evaporites).

These models highlight the critical factors that can induce folding in extension.

(1) The presence of a thick "viscous" layer allows a vertical decoupling between block faulting in basement and flexure of the cover. This corresponds to the relatively incompetent succession of Lower Dogger, Lias and Trias (about 800 m thick) dominated by marls and evaporites.

(2) A low displacement rate on controlling faults promotes fault-propagation folding as suggested by analogue models of Withjack and Callaway (2000). In the Dannemarie basin, the period during which most of the fault-related folds formed corresponds to the Salt Series. The age of this series, which is on average 1300 m thick, is unfortunately not well constrained. Based on Berger et al. (2005a), it was deposited from Lutetian to Middle Rupelian, a period of 12 Myr. For the same period, slip along faults estimated from FaultFold models was between 1200 m and 1450 m (Table 1), which yields a displacement rate of between 100 and 120 m/Myr (0.1–0.12 mm/yr). Even if the age of the base of the LSF is taken as late Priabonian (35 Ma), the displacement rate increases to between 266 and 322 m/Myr (0.26–0.33 mm/yr).

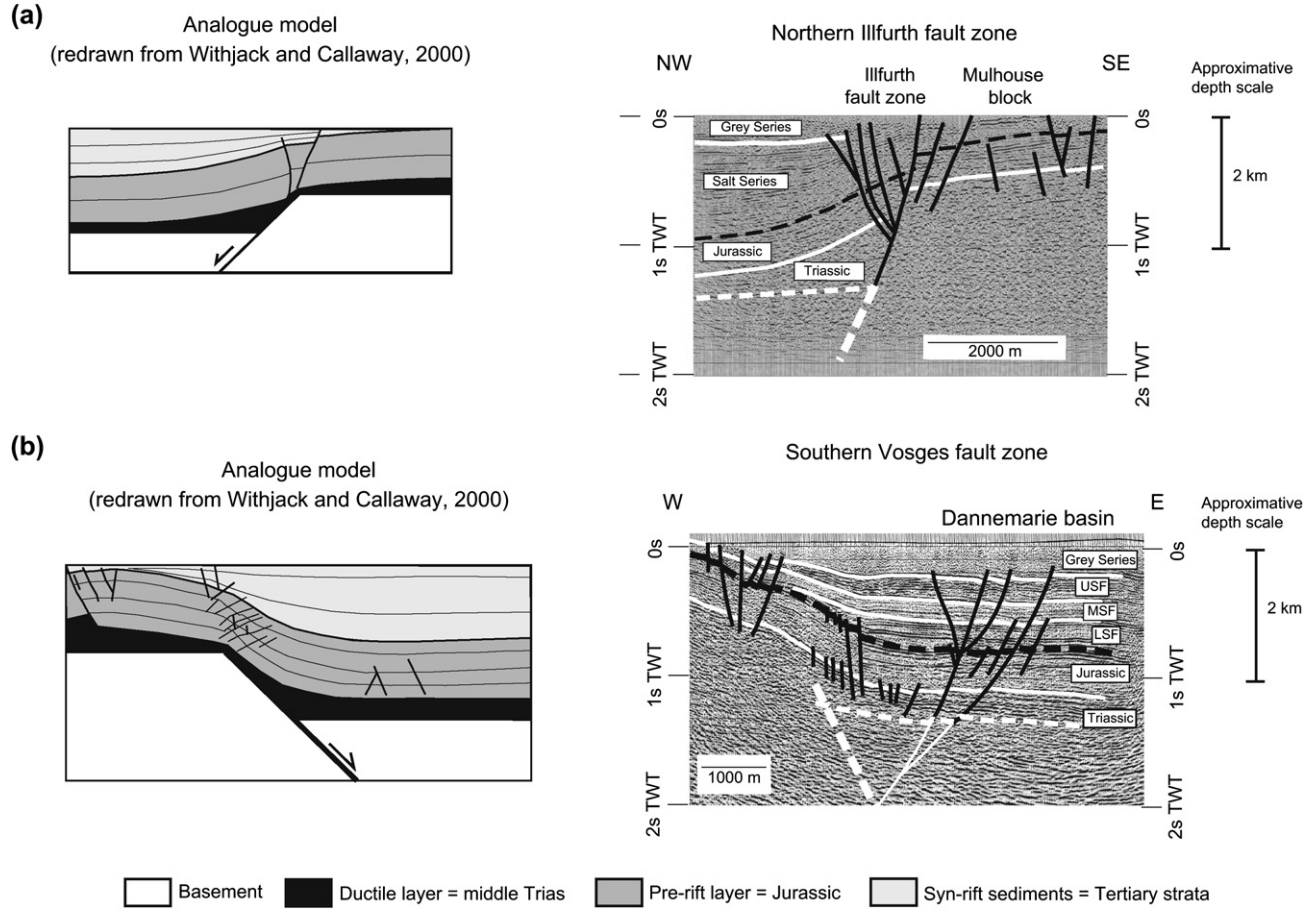


Fig. 12. Comparison between analogue models of Withjack and Callaway (2000) with (a) the structure of the northern Illfurth fault zone and monocline (Fig. 5d), and (b) the Felon flexure at the southern end of the Vosges fault zone (Fig. 4d). Based on the analogue models, the probable trace of top basement and the basement fault have been added each section (white dashed lines).

These are relatively slow displacement rates for normal faults (Nicol et al., 1997).

### 4.3. The trishear model

While the parameters of the 'best fit' trishear models are relatively constant for all three cross-sections (Table 1), their geological significance and validity requires consideration. Only one fault can be active at any one time in the trishear model. Observed onlap of the Salt formations dictates that the most basin-ward fault was active first (LSF). Deformation then migrated into its footwall onto the principal fault zone (MSF and USF; see Table 1 and Figs. 9–11).

In trishear models, the P/S ratio can be seen as a proxy for the strength distribution in cover stratigraphy (Hardy and McClay, 1999). The P/S ratio of 0, necessary to generate the observed folds during early rifting, has a significant impact on the geometry of beds and on the distribution of strain. Stretching occurs on the monoclinal limb while the lowest unit above faulted basement shows significant thickness variations, which can only be explained by a viscous rheology (compare with Fig. 12). While the faulted nature of competent units on monocline limbs appears to support these models, the poor resolution of seismic lines prohibits a detailed analysis of limb strain, which would allow a closer comparison with strain distribution predicted in trishear models (Allmendinger, 1998; Hardy and McClay, 1999).

The best fit trishear angle of 120° is the same as that used to model extensional fault-related folds in the NW Red Sea with Faultfold software (Khalil and McClay, 2002). In both studies the initial fault tip was assumed to be located at the top of basement. If the tip points were deeper (for example, in the URG due to the presence of Permian grabens (Ustaszewski et al., 2005)) the trishear angle necessary to reproduce observed fold geometries would decrease (ca. 90°). In contrast, the non-linear trishear model of Jin and Groshong (2006) predicts much lower apical angles (to ca. 50–60°) to replicate similar analogue modelling and natural extensional folds. We did not apply this model because we could not measure with certainty deformed hangingwall and footwall apical angles.

This study suggests that several close faults might have been active at the same time, with overlapping deformation areas. With this kind of configuration, and within the limitations of the FaultFold program (only one fault active at one time), it would be necessary to artificially enlarge the trishear angle to fit at the first-order the observed geometries. From this point of view, the initial tip location is a key parameter when performing forward trishear modelling. Uncertainty in the location of the fault tip will generate a range of acceptable models, with significant implications for other trishear parameters.

While the trishear approach is a useful tool for modelling extensional fault-related folds in the URG, several limitations must be noted. Firstly, only one fault can be active at any one time. Secondly, as the model is 2D, the importance of oblique movements cannot be considered. Thirdly, no rheological parameters can be incorporated.

Recent mechanical modelling of fault-related folds (contractional or extensional) has demonstrated a first-order control of deformation by rheological layering in the stratigraphy (Finch et al., 2004; Hardy and Finch, 2006). For example, when incompetent layers are relatively thick, deformation is not restricted to a triangular zone emanating from the fault tip, but can be more widely distributed along competent layers in the proto-footwall and proto-hangingwall. Analogue models (Withjack et al., 1990; Withjack and Callaway, 2000) also indicate that the presence of a thick viscous layer may promote the initiation of new faults disconnected from the initial basement fault, therefore inhibiting its propagation upward through its flexure (Fig. 12b). Detached grabens may form in the hangingwall as well as in the footwall of the main fault (Withjack and Callaway, 2000; Jackson et al., 2006). As noted above, these phenomena are observed in the URG (Fig. 4b).

## 5. Conclusions

This 3D study demonstrates that subsidence in the URG Dannemarie basin was controlled by normal faults associated with significant syn-rift monoclines. These monoclines are interpreted as fault-propagation folds that developed above upward-propagating normal faults, which themselves were probably re-activated basement faults. The 3D model for the Dannemarie basin clarifies lateral variations in fault-fold relations along basin margins and the geometry of syn-rift infill, avoiding misinterpretation of geometries due to non-linear seismic profiles. While the trishear model is a useful tool with which to replicate the early syn-rift folds of the Dannemarie basin, it may not fully represent the true distribution of strain during early rifting. Progressive unfolding of the 3D model in gOcad will provide an inverse model of strain distribution across the basin at different stages of rifting.

Extensional fault-related folds tend to develop during the early stages of rifting. They are particularly well preserved in the Dannemarie basin because rifting was terminated abruptly at the end of the Chattian, probably due to the arrival of the Alpine forebulge (Gutscher, 1995; Bourgeois et al., in press). As shown in the Guebwiller cross-section, once a fold is breached, displacement is accommodated on planar faults. Late listric faulting may also develop. The presence of significant volumes of border conglomerates along the Vosges margin indicates that major breaching faults were also active to the west of the flexure zone, creating footwall relief. Extensional fault-related folds therefore accommodate a relatively early and often significant component of regional extensional strain.

The ubiquitous occurrence of these syn-rift folds around the Dannemarie basin can be explained by the coincidence of a number of favourable conditions, in particular the presence of favourably oriented basement faults, a thick viscous layer allowing vertical decoupling between basement and cover, and finally, a low deformation rate. The absence of syn-rift folds along strike to the north suggests that structural style can change along normal fault zones due to lateral heterogeneity in, for example, lithostratigraphy or deformation

rate. Similar lateral variations have been observed by Jackson et al. (2006) in the Suez Rift. The critical range of values of controlling parameters, their relative importance and combinations necessary to allow the development of extensional folds have yet to be clearly delineated. However, the large number of detailed case studies and developments in modelling in the last decade have greatly advanced our understanding of these folds. These studies have economic implications as they impact on hydrocarbon exploration in rift basins.

## Acknowledgements

The authors thank the directors of the GéoFrance 3D program ''Fossé Rhénan'' (Thierry Winter and Patrick Ledru), the BRGM (Philippe Elsass) and the EOST (Marc Schaming) for access to seismic and borehole data. The Région Lorraine and the BRGM are acknowledged for their financial support. This work benefited from fruitful discussions with members of GéoFrance3D ''Fossé Rhénan'' and the EUCOR-URGENT research groups. We thank Martha Withjack and Rick Groshong for their constructive reviews. Contribution CRPG n°1855.

## References

Allmendinger, R., 1998. Inverse and forward numerical modeling of trishear fault-propagation folds. Tectonics 17 (4), 640–656.

Allmendinger, R.W., Zapata, T.R, Manceda, R., Dzelalija, F., 2004. Trishear kinematic modeling of structures with examples from the Neuquén basin, Argentina. In: McClay, K.R. (Ed.), Thrust Tectonics and Hydrocarbon Systems: AAPG Memoir 82. American Association of Petroleum Geologists, Tulsa, pp. 356–371.

Berger, J.P., Reichenbacher, B., Becker, D., Grimm, M., Grimm, K., Picot, L., Storni, A., Pirkenseer, C., Derer, C., Schaefer, A., 2005a. Paleogeography of the Upper Rhine Graben (URG) and the Swiss Molasse Basin (SMB) from Eocene to Pliocene. International Journal of Earth Sciences 94, 697–710.

Berger, J.-P., Reichenbacher, B., Becker, D., Grimm, M., Grimm, K., Picot, L., Storni, A., Pirkenseer, C., Schaefer, A., 2005b. Eocene-Pliocene time scale and stratigraphy of the Upper Rhine Graben (URG) and the Swiss Molasse Basin (SMB). International Journal of Earth Sciences 94, 711–731.

Bergerat, F., 1987. Stress fields in the European platform at the time of Africa-Eurasia collision. Tectonics 6, 99–132.

Brun, J.-P., Gutscher, M.-A., DEKORP-ECORS teams, 1992. Deep crustal structure of the Rhine Graben from DEKORP-ECORS seismic reflection data: a summary. Tectonophysics 208, 139–147.

Bourgeois, O., Diraison, M., Le Carlier de Veslud, C., Ford, M., 2004. Geodynamic controls on the Cenozoic-Pleistocene development of the southern Upper Rhine Graben, Réunion des Sciences de la Terre, Strasbourg, Abstract.

Bourgeois, O., Ford, M., Diraison, M., Le Carlier de Veslud, C., Gerbault, M., Pik, R., Ruby, N., Bonnet S. Separation of rifting and lithospheric folding signatures in the NW-Alpine foreland. International Journal of Earth Sciences, in press, doi:10.1007/s00531-007-0202-2.

Derer, C., Schumacher, M., Schäfer, A., 2005. The northern Upper Rhine Graben: basin geometry and early syn-rift tectono-sedimentary evolution. International Journal of Earth Sciences 94 (4), 640–656.

Duringer, P., 1988. Les conglomérats des bordures du rift cénozoïque rhénan. Dynamique sédimentaire et contrôle climatique. Unpublished PhD. Thesis, Université Louis Pasteur, Strasbourg.

Edel, J.B., Lutz, H., Elsass, P., 2002. Socle varisque et tectoniques rhénanes dans le Fossé rhénan supérieur méridional: traitement et interprétation de la carte gravimétrique du fossé à partir du levé haute densité des MPDA. Géologie de la France 3, 43–59.

Edel, J.-B., Schulmann, K., Rotstein, Y., 2007. The Variscan tectonic inheritance of the Upper Rhine Graben: evidence of reactivations in the Lias, Late Eocene-Oligocene up to the recent. International Journal of Earth Sciences, doi:10.1007/s00531-006-0092-8.

Erslev, E., 1991. Trishear fault-propagation folding. Geology 19 (6), 617–620.

Finch, E., Hardy, S., Gawthorpe, R., 2004. Discrete-element modelling of extensional fault-propagation folding above rigid basement fault blocks. Basin Research 16, 489–506.

Gawthorpe, R.L., Jackson, C.A.L., Young, M.J., Sharp, I.R., Moustafa, A.R., Leppard, C.W., 2003. Normal fault growth, displacement localisation and the evolution of normal fault populations: the Hammam Faraun fault block, Suez rift, Egypt. Journal of Structural Geology 25, 883–895.

Giamboni, M., Ustaszewski, K., Schmid, S.M., Schumacher, M.E., Wetzel, A., 2004. Plio-Pleistocene transpressional reactivation of Paleozoic and Paleogene structures in the Rhine-Bresse transform zone (northern Switzerland and eastern France). International Journal of Earth Sciences 93, 207–223.

Gutscher, M.-A., 1995. Crustal structures and dynamics in the Rhine Graben and Alpine foreland. Geophysical Journal International 122, 617–636.

Hardy, S., Finch, E., 2006. Discrete element modelling of the influence of cover strength on basement-involved fault-propagation folding. Tectonophysics 415, 225–238.

Hardy, S., Ford, M., 1997. Numerical modeling of trishear fault-propagation folding. Tectonics 16, 841–854.

Hardy, S., McClay, K., 1999. Kinematic modelling of extensional fault-propagation folding. Journal of Structural Geology 21, 695–702.

Hinskin, S., Ustazewski, K., Wetzel, A. Graben width controlling syn-rift sedimentation: the Paleogene southern Upper Rhine Graben as an example, International Journal of Earth Sciences in press, doi:10.1007/s00531-006-0162-y.

Illies, J.H., 1975. Recent and paleo-intraplate tectonics in stable Europe and Rheingraben rift system. Tectonophysics 29, 251–264.

Jackson, C.A.L., Gawthorpe, R.L., Sharp, I.R., 2006. Style and sequence of deformation during extensional fault-propagation folding: examples from the Hammam Faraun and El-Qaa fault blocks, Suez Rift, Egypt. Journal of Structural Geology 28, 519–535.

Jin, G., Groshong Jr., R.H., 2006. Trishear kinematic modeling of extensional fault-propagation folding. Journal of Structural Geology 28, 170–183.

Keller, J.V.A., Lynch, G., 1999. Displacement transfer and forced folding in the Maritimes Basin of Nova Scotia, Eastern Canada. In: Cosgrove, J.W., Ameen, M.S. (Eds.), Forced Folds and Fractures. Geological Society, Special Publications, London, 169, pp. 73–86.

Khalil, S.M., McClay, K.R., 2002. Extensional fault-related folding, northwestern Red Sea, Egypt. Journal of Structural Geology 24, 743–762.

Larroque, J.M., Ansart, M., 1985. Les déformations liées à la tectonique distensive oligocene du bassin potassique de Mulhouse; cas du secteur minier. Bulletin de la Société Géologique de France. Huitieme Serie 1, 837–847.

Laubscher, H., 1982. Die Sudostecke des Rheingrabens. Ein kinematisches und dynamisches problem. Eclogae Geologicae Helvetiae 75, 101–116.

Laubscher, H., 2001. Plate interactions at the southern end of the Rhine Graben. Tectonophysics 343, 1–19.

Le Carlier de Veslud, C., Ford, M., Bourgeois, O., Diraison, M., 2005. 3D Stratigraphic and structural synthesis of the Dannemarie Basin (Upper Rhine Graben). Bulletin de la Société Géologique de France 176 (5), 433–442.

Lutz, M., Cleintuar, M., 1999. Geological results of a hydrocarbon exploration campaign in the southern Upper Rhine Graben. VSP/SFIG Bulletin for Applied Geology 4 (Suppl. 1999), 3–80.

Mallet, J.L., 2002. Geomodeling. Oxford University Press, 624 p.

Maurin, J.C., 1995. Drapage et décollement des séries jurassiques sur la faille de détachement majeur du rift rhénan sud: implications sur la géométrie des dépôts syn-rifts oligocènes. Comptes Rendus de l'Académie des Sciences. série IIa, 321, 1025–1032.

Maurin, J.C., Nivière, B., 2000. Extensional forced folding and décollement of the pre-rift series along the Rhine graben and their influence on the geometry of the syn-rift sequences. In: Cosgrove, J.W., Ameen, M.S (Eds.), Forced Folds and Fractures. Geological Society, Special Publications, London, 169, pp. 73–86.

Merle, O., Michon, L., 2001. The formation of the West European rift: a new model as exemplified by the Massif Central area. Bulletin de la Société Géologique de France 172, 213–221.

Nicol, A., Walsh, J.J., Watterson, J., Underhill, J.R., 1997. Displacement rates of normal faults. Nature 390, 157–159.

Nivière, B., Winter, T., 2000. Pleistocene northwards fold propagation of the Jura within the southern Upper Rhine Graben: seismotectonic implications. Global and Planetary Change 27, 263–288.

Paton, D., Underhill, J.R., 2004. Role of crustal anisotropy in modifying the structural and sedimentological evolution of extensional basins: the Gamboos Basin, South Africa. Basin Research 16, 339–359.

Rotstein, Y., Schaming, M., Rousse, S., 2005a. Tertiary tectonics of the Dannemarie Basin, Upper Rhine Graben, and regional implications. International Journal of Earth Sciences 94, 669–679.

Rotstein, Y., Behrmann, J.H., Lutz, M., Wirsing, G., Luz, A., 2005b. Tectonic implications of transpression and transtension: Upper Rhine Graben, Tectonics, 24, TC6001, doi:10.129/2005TC001797.

Schumacher, M., 2002. Upper Rhine Graben: role of pre-existing structures during rift evolution. Tectonics 21, 6–1-6-17.

Sharp, I.R., Gawthorpe, R.L., Underhill, J., Gupta, S., 2000. Fault-propagation folding in extensional settings: examples of structural style and synrift sedimentary response from the Suez rift, Sinai, Egypt. Geological Society of America Bulletin 112 (12), 1877–1899.

Sissingh, W., 1998. Comparative Tertiary stratigraphy of the Rhine Graben, Bresse Graben and Molasse Basin: correlation of Alpine foreland events. Tectonophysics 300, 249–284.

Sissingh, W., 2003. Tertiary paleogeographic and tectonostratigraphic evolution of the Rhenish Triple Junction. Palaeogeography, Palaeoclimatology. Palaeoecology 196, 229–263.

Sittler, C., 1969. Le fossé rhénan, Alsace. Aspect structural et histoire géologique. Revue de Géologie Dynamique et de Géographie Physique 11, 465–494.

Sittler, C., 1983. Le fossé rhénan. In: Encyclopédie de l'Alsace, 5. Strasbourg. 3122–3137.

Theobald, N., 1977. Neuf-Brisach-Obersaasheim, BRGM 1:50 000 geological map, 378–379, Bureau de Recherches Géologiques et Minières.

Theobald, N., Devantoy, J., 1963. Belfort, 1:50 000 geological map, 444, Bureau de Recherches Géologiques et Minières.

Ustaszewski, K., Schumacher, M., Schmid, S., 2005. Simultaneous normal faulting and extensional flexuring during rifting: an example from the southernmost Upper Rhine Graben. International Journal of Earth Sciences 94, 680–697.

Vendeville, B., Hongxing, G., Jackson, M.P.A., 1995. Scale models of salt tectonics during basement-involved extension. Petroleum Geoscience 1, 179–183.

Villemin, T., Bergerat, F., 1987. L'évolution structurale du fossé rhénan au cours du cénozoïque: un bilan de la déformation et des effets thermiques de l'extension. Bulletin de la Societé Géologique de France 3, 245–255.

Villemin, T., Alvarez, F., Angelier, J., 1986. The Rhinegraben; extension, subsidence and shoulder uplift. Tectonophysics 128 (1–2), 47–59.

Withjack, M., Callaway, S., 2000. Active normal faulting beneath a salt layer: an experimental study of deformation patterns in the cover sequence. American Association of Petroleum Geologists Bulletin 84, 627–651.

Withjack, M.O., Òlson, J., Peterson, E., 1990. Experimental models of extensional forced folds. American Association of Petroleum Geologists Bulletin 74, 1038–1054.

Young, M., Gawthorpe, R., Hardy, S., 2001. Growth and linkage of a segmented normal fault zone; the Late Jurassic Murchison-Statfjord North Fault, northern North Sea. Journal of Structural Geology 23, 1933–1952.

Zehnder, A., Allmendinger, R., 2000. Velocity field for the trishear model. Journal of Structural Geology 22, 1009–1014.

Ziegler, P.A., 1992. European Cenozoic rift system. Tectonophysics 208. 91–111.

Ziegler, P.A., Dezes, P., 2005. Evolution of the lithosphere in the area of the Rhine Rift System. International Journal of Earth Sciences 94, 594–614.